JIPB Journal of Integrative Plant Biology

Research Article
https://doi.org/10.1111/jipb.13402

Rice *FLOURY ENDOSPERM22*, encoding a pentatricopeptide repeat protein, is involved in both mitochondrial RNA splicing and editing and is crucial for endosperm development

Hang Yang[1†], Yunlong Wang[1†], Yunlu Tian[1†], Xuan Teng[1], Zehui Lv[1], Jie Lei[1], Erchao Duan[1], Hui Dong[1], Xue Yang[1], Yuanyan Zhang[1], Yinglun Sun[1], Xiaoli Chen[1], Xiuhao Bao[1], Rongbo Chen[1], Chuanwei Gu[1], Yipeng Zhang[1], Xiaokang Jiang[1], Wenyu Ma[1], Pengcheng Zhang[1], Yi Ji[1], Yu Zhang[1], Yihua Wang[1]* and Jianmin Wan[1,2]*

1. State Key Laboratory for Crop Genetics and Germplasm Enhancement, Jiangsu Plant Gene Engineering Research Center, Nanjing Agricultural University, Nanjing 210095, China

2. National Key Facility for Crop Resources and Genetic Improvement, Institute of Crop Sciences, Chinese Academy of Agricultural Sciences, Beijing 100081, China

†These authors contributed equally to this work.

*Correspondences: Jianmin Wan (wanjm@njau.edu.cn, Dr. Wan is fully responsible for the distributions of all materials associated with this article); Yihua Wang (yihuawang@njau.edu.cn)

Hang Yang

Jianmin Wan

ABSTRACT

Most of the reported P-type pentatricopeptide repeat (PPR) proteins play roles in organelle RNA stabilization and splicing. However, P-type PPRs involved in both RNA splicing and editing have rarely been reported, and their underlying mechanism remains largely unknown. Here, we report a rice *floury endosperm22* (*flo22*) mutant with delayed amyloplast development in endosperm cells. Map-based cloning and complementation tests demonstrated that *FLO22* encodes a mitochondrion-localized P-type PPR protein. Mutation of FLO22 resulting in defective *trans*-splicing of mitochondrial *nad1* intron 1 and perhaps causing instability of mature transcripts affected assembly and activity of complex I, and mitochondrial morphology and function. RNA-seq analysis showed that expression levels of many genes involved in starch and sucrose metabolism were significantly down-regulated in the *flo22* mutant compared with the wild type, whereas genes related to oxidative phosphorylation and the tricarboxylic acid cycle were significantly up-regulated. In addition to involvement in splicing as a P-type PPR protein, we found that FLO22 interacted with DYW3, a DYW-type PPR protein, and they may function synergistically in mitochondrial RNA editing. The present work indicated that FLO22 plays an important role in endosperm development and plant growth by participating in *nad1* maturation and multi-site editing of mitochondrial messager RNA.

Keywords: endosperm development, *Oryza sativa*, PPR proteins, RNA editing, RNA splicing

Yang, H., Wang, Y., Tian, Y., Teng, X., Lv, Z., Lei, J., Duan, E., Dong, H., Yang, X., Zhang, Y., Sun, Y., Chen, X., Bao, X., Chen, R., Gu, C., Zhang, Y., Jiang, X., Ma, W., Zhang, P., Ji, Y., Zhang, Y., Wang, Y., and Wan, J. (2022). Rice *FLOURY ENDOSPERM22*, encoding a pentatricopeptide repeat protein, is involved in both mitochondrial RNA splicing and editing and is crucial for endosperm development. J. Integr. Plant Biol. **00:** 1–18.

INTRODUCTION

The endosperm of cereal grains is a major carbon source due to the storage of large amounts of starch (Liu et al., 2022). In rice, starch is mainly synthesized in amyloplasts of central endosperm cells through a series of complex enzymes such as adenosine diphosphate glucose pyrophosphorylase (AGPase) (James et al., 2003). Mutations

of these starch biosynthesis related enzymes usually lead to abnormal endosperm (Fujita et al., 2007; Kawagoe et al., 2010; Toyosawa et al., 2016). Several genes indirectly influencing starch accumulation have been characterized in the past decade (Peng et al., 2014; Long et al., 2018; Hao et al., 2019; Wu et al., 2019). Mutations in these genes cause incomplete starch filling in the grain, resulting in partial or entire opaqueness of mature seeds. These studies revealed that starch synthesis involves a variety of physiological and biochemical processes, and indicated that more novel regulators remained to be identified.

Mitochondria, as semiautonomous organelles, widely exist in eukaryotes. These organelles convert chemical energy into adenosine triphosphate (ATP) through electron transport chains (ETC), which are used directly for a variety of cellular activities. Defects in mitochondrial function often have dramatic effects on plant growth and development (Liu et al., 2013; Yang et al., 2017). Although possessing a genome harboring ~50 protein-coding genes, many nuclear-encoded proteins are required to regulate mitochondrial gene expression (Barkan and Small, 2014). Diverse nuclear-encoded proteins, including pentatricopeptide repeat (PPR) proteins, plant organelle RNA recognition motif proteins and multiple organellar RNA editing factors, participate in regulating mitochondrial genes in processes like RNA processing, decay, editing and intron splicing at the post-transcriptional RNA level (Sun et al., 2016; Small et al., 2020).

PPR proteins, characterized by the presence of tandem degenerate motifs of PPR repeats, form a huge family consisting of over 400 members in land plants (Lurin et al., 2004; Barkan and Small, 2014). The vast majority are targeted to mitochondria or chloroplasts, or both, and have sequence-specific binding activity in these organelles (Barkan and Small, 2014; Andres-Colas et al., 2017). PPR proteins are further divided into P and PLS subfamilies according to amino acid conservation and function. P-type PPR proteins contain only canonical 35-amino acid PPR motifs, whereas PLS-type PPR proteins comprise P, L (long, 35-36 amino acids), and S (short, 31 amino acids) PPR motifs. In addition, some PLS-type PPR proteins have E, E^+, and DYW domains at the C-terminus that are essential for RNA recognition and editing (Chateigner-Boutin et al., 2013). P subfamily proteins are mainly involved in RNA splicing, cleavage, stabilization, and translation initiation (Cai et al., 2011; Chen et al., 2017; Wu et al., 2019), whereas PLS subfamily proteins generally function in C-to-U editing in mitochondria and chloroplasts (Cai et al., 2009; Brehme et al., 2015). The ability of P-type PPR proteins to bind RNA is an important mechanism for the nucleus to regulate organelle gene expression by promoting the maturation of RNAs and the maintenance of the stability of transcripts (Barkan and Small, 2014). In angiosperm mitochondria and plastids there are approximately 500 and 30 sites, respectively, at which there is C-to-U editing (Small et al., 2020). These base changes in semiautonomous organelles usually restore conserved codons or form new start and stop codons, working as a correction mechanism (Fujii and Small, 2011; Sun et al., 2016; Small et al., 2020). In addition, multiple PPR proteins can cooperatively participate in the RNA editing process in mitochondria and plastids (Chateigner-Boutin et al., 2008; Guillaumot et al., 2017). In *Arabidopsis*, an E^+-type PPR protein SLO2 which does not have a DYW domain, recruits a DYW-type protein DYW2 and a P-type PPR protein NUWA for a complete editing event in mitochondria (Andres-Colas et al., 2017). Simultaneously, an E^+-type PPR protein CLB19 without DYW domain, interacting with NUWA and DYW2, is responsible for multi-site RNA editing in plastids (Guillaumot et al., 2017). To date, no PPR protein complex involved in RNA editing has been reported in rice.

PPR proteins play important roles in respiration, photosynthesis, biotic and abiotic stress, pollen fertility, leaf and seed development (Ding et al., 2006; Johnson et al., 2010; Bryant et al., 2011; Zsigmond et al., 2012; Liu et al., 2013; Chen et al., 2017; Hao et al., 2019; Wu et al., 2019). For example, *FLOURY ENDOSPERM10 (FLO10)* encodes a P-type PPR protein that is required for the *trans*-splicing of the mitochondrial *nad1* intron1, and its mutation led to a decreased activity of mitochondrial respiratory complex I, and affected endosperm development in rice (Wu et al., 2019). Moreover, OGR1, MPR25 and EMP5 were found to participate in mitochondrial RNA editing and are important for seed development (Kim et al., 2009; Toda et al., 2012; Li et al., 2014). However, there are few reports about collaboration of multi-type PPR proteins in RNA editing and how they affect endosperm development.

In this study, we report a *flo22* mutant which has smaller starch grains (SGs) and compromised plant growth. *FLO22* encodes a mitochondrion-localized P-type PPR protein which is responsible for the formation of mature *nad1*. It also interacts with DYW-type PPR protein DYW3 and possibly PLS31 and PLS33 and might be involved in the editing of multiple mitochondrial transcript sites. Our results reveal that FLO22 is essential for RNA processing of mitochondrial transcripts, especially members of respiration complex I, which is important for endosperm development and plant growth in rice.

RESULTS

Isolation and characterization of the *flo22* mutant

Screening of the N-methyl-N-nitrosourea (MNU)-treated *indica* variety N22 led to isolation of mutant *flo22* with opaque, entirely floury mature grains (Figure 1A–D). The plant height of the mutant was significantly less than the wild type at both the seedling (Figure S1A) and heading (Figures 1E, S1B) stages. The *flo22* mutant exhibited slower dry matter accumulation during grain filling (Figure 1F). There was no difference in the seed setting rate (Figure S1C). Scanning electron microscopy (SEM) of mature grains showed that starch granules in mutant endosperm cells were loosely packed and rounder (Figure 1H, J), whereas endosperm cells

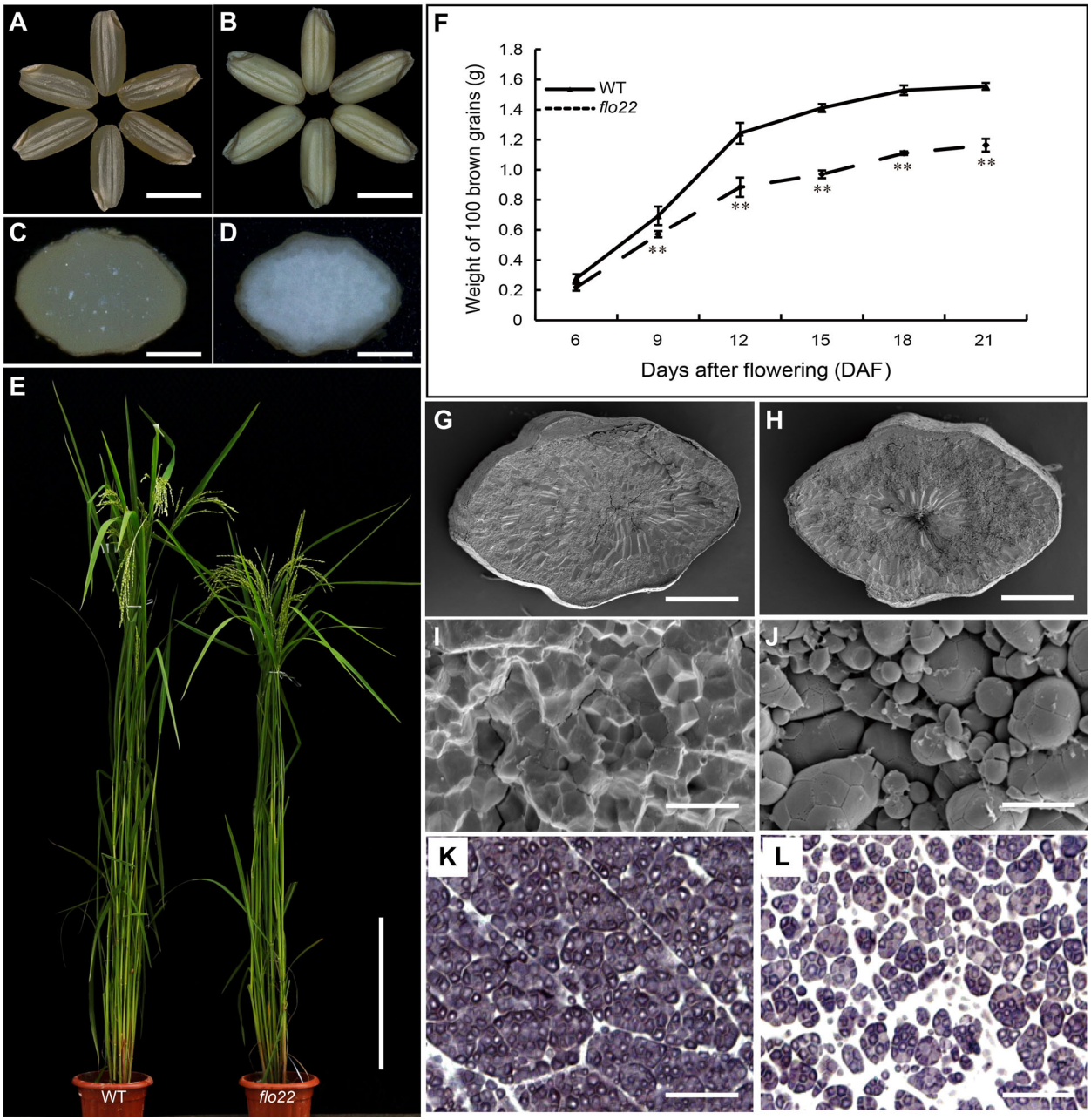

Figure 1. The *floury endosperm22* (*flo22*) mutant exhibits defective endosperm development and plant growth

(**A**, **B**) Mature seeds of wild type N22 (**A**) and the *flo22* mutant (**B**); bars, 5 mm. (**C**, **D**) Cross-sections of wild type (**C**) and *flo22* mutant (**D**) seeds; bars, 1 mm. (**E**) Plant heights of wild type and *flo22* mutant after heading; bar, 40 cm. (**F**) Grain filling of wild type and the *flo22* mutant at different stages of endosperm development. Scanning electron microscope images of transverse sections of wild type (**G**, **I**) and *flo22* mutant (**H**, **J**) seeds; bars, 1 mm in (**G**, **H**), 10 μm in (**I**, **J**). (**K**, **L**) Central parts of 9 DAF wild type (**K**) and *flo22* mutant (**L**) endosperm cells stained with iodine-potassium iodide (I2-KI); bars, 100 μm. DAF, d after flowering.

in the wild type were fully filled with compact starch granules (Figure 1G, I). Iodine staining semithin sections of developing endosperm at 9 d after flowering (DAF) showed that the mutant had smaller SGs with lots of gaps (Figure 1K, L) compared with the wild type. Thousand-grain weight was significantly reduced by about 17% (Figure S1E). Total starch and amylose contents in the mutant were significantly less than in the wild type (Figure S1F, G), whereas lipid content was increased (Figure S1H). Together, these results indicated that the *flo22* mutation caused defective endosperm starch synthesis and retarded plant growth.

Map-based cloning of the *FLO22* locus

Based on 10 floury individuals selected from the F_2 population of Ninggeng 4 (NG4) crossed to the *flo22* mutant the *FLO22* locus was initially mapped to a 16 cM region flanked

by simple sequence repeat marker N7-4 and InDel marker I7-3 on chromosome 7. The mapped interval was then fine mapped to a 170 kb region flanked by markers 7F-12 and JRN7-19 using 1,000 F_2 individuals (Figure 2A). Fourteen open reading frames in this region were each polymerase chain reaction (PCR)-amplified for sequencing. A single base substitution of adenine (A) to thymine (T) at position 611 in *LOC_Os07g08180* caused an amino acid change of histidine (His) to leucine (Leu). The mutation occurs in a helix structure (Figure 2B).

To investigate whether *LOC_Os07g08180* was the *FLO22* gene, we performed a complementation test by introducing fusion construct pCAMBIA1300-221- LOC_Os07g08180*3flag to *flo22* mutant calli. All the positive transgenic plants restored seedling growth rate and plant height (Figure S2A–D) and produced transparent mature grains resembling those of the wild type (Figure 2C). We concluded that the mutation in *LOC_Os07g08180* was responsible for the defective phenotype of the *flo22* mutant. To determine the effect of the mutation, we examined FLO22 protein levels in wild type and *flo22* mutant at different stages of endosperm development. It was found that the protein levels of FLO22 were slightly elevated in the mutant (Figure 2D).

FLO22 was predicted to encode a P-type PPR protein with 11 canonical P repeats and 2 S repeats (Figure 2B). It shared high sequence similarity in PPR motifs with homologous proteins (Figure S3A, B). Amino acid sequence alignment showed the mutation occurred in a His site that was conserved in all analyzed plant species (Figure S3A).

Expression pattern of *FLO22* and subcellular localization of FLO22

FLO22 was constitutively expressed in all examined tissues including roots, leaf sheaths, leaves, stems, panicles, and developing endosperm. Expression of *FLO22* was higher in leaves, panicles and leaf sheaths, and increased in seeds from 9 DAF to 18 DAF representing the middle stage of endosperm development (Figure 3A).

TargetP prediction of FLO22 did not indicate the presence of mitochondrial or chloroplast transit peptides. To determine the subcellular location of FLO22, pCAMBIA1305-FLO22-GFP (green fluorescent protein) and pAN580-FLO22-GFP

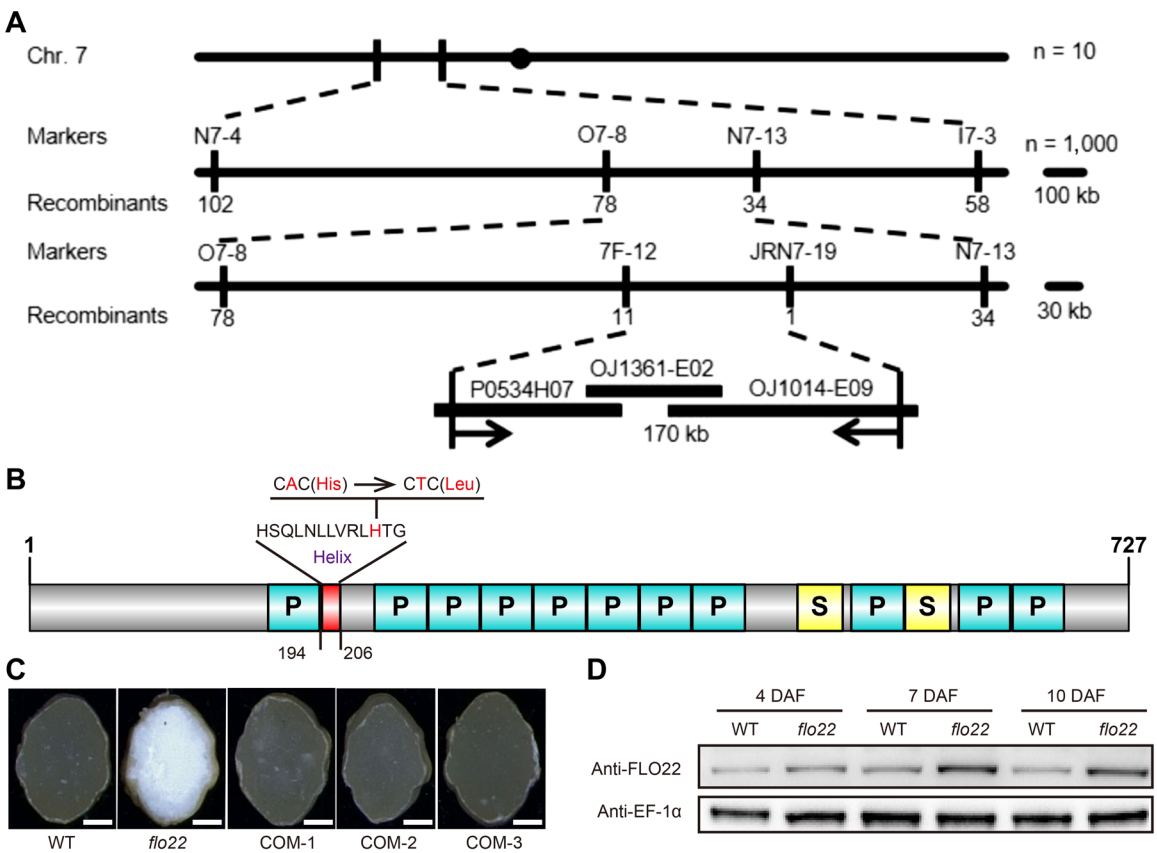

Figure 2. Map-based cloning and complementation test of *FLOURY ENDOSPERM22* (*FLO22*)

(**A**) *FLO22* was located in a 170 kb region of chromosome 7 using 1,000 individuals. (**B**) The *flo22* mutant has a single base change from A to T in the 611th nucleotide of the coding region of *LOC_Os07g08180*, leading to a His to Leu change in the 204th amino acid. His, histidine; Leu, leucine. Analysis of the secondary structure of the *FLO22* amino acid revealed that the mutation occurred in one helix (https://predictprotein.org/). The FLO22 protein contains 13 pentatricopeptide repeat (PPR) motifs. P, PPR repeat with 35 amino acids, S, short PPR repeat with 31 amino acids. (**C**) Cross-sections of mature grains of wild type, *flo22* mutant, and complementary lines (COM1-COM3). Bars, 0.5 mm. (**D**) Immunoblotting of FLO22 at different stages of endosperm development. Anti-EF-1α antibodies were used as a loading control.

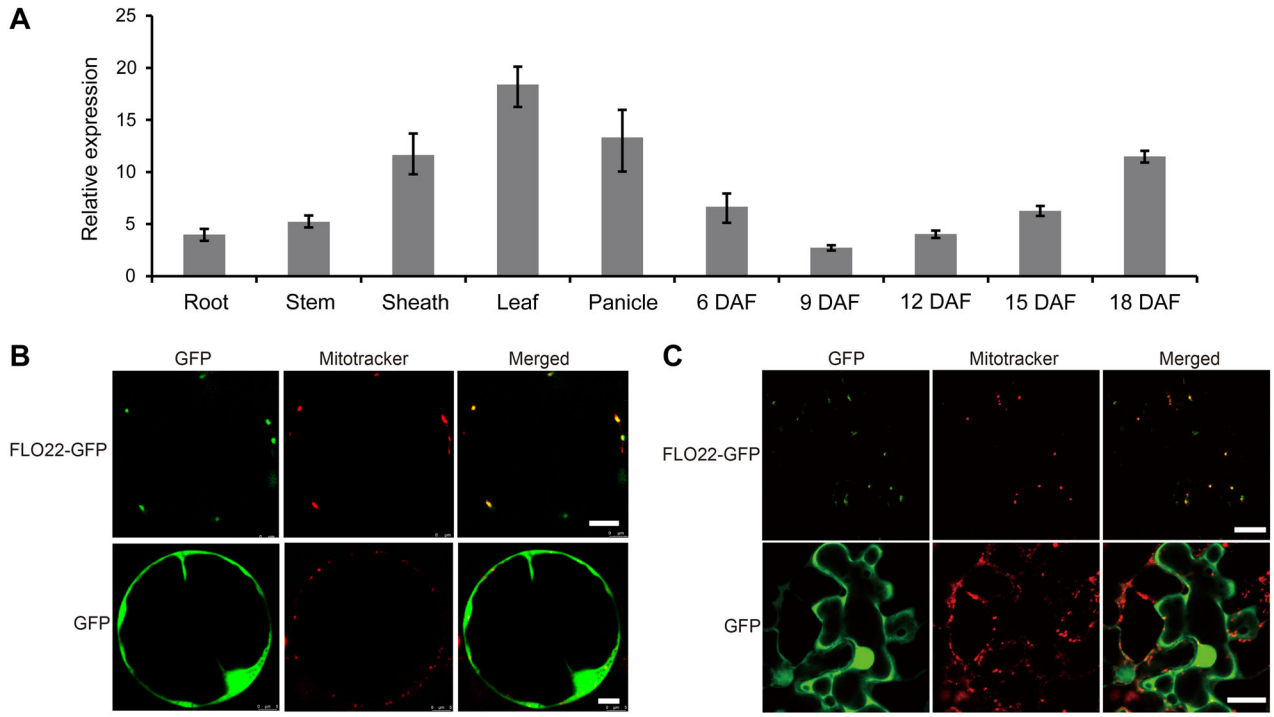

Figure 3. Expression pattern analysis of *FLOURY ENDOSPERM22* (*FLO22*) and subcellular localization of FLO22

(**A**) Expression levels of *FLO22* in the various tissues and different developmental stages of endosperm in the wild type. *UBIQUITIN* was used as an internal control. Values are means ± *SD* ($n = 3$). DAF, days after flowering. (**B**, **C**) Localization of FLO22-GFP (green fluorescent protein) fusion protein in rice protoplasts (**B**) and *Nicotiana benthamiana* leaf epidermal cells (**C**). Mito-Tracker Orange CM-H2TMRos (Invitrogen) was injected into the *N. benthamiana* leaves or added into the protoplast suspension to dye the mitochondria for 30 min. Bars, 5 μm in (**B**); 25 μm in (**C**)

fusion constructs were transformed into tobacco leaf epidermal cells and rice protoplasts, respectively. Signals of FLO22-GFP fusion protein in both systems overlapped well with the fluorescence from mitochondria dye Mito-Tracker Orange (Figure 3B, C), whereas the signal of free GFP was distributed in the cytosol and nucleus. This showed that FLO22 was a mitochondrion-localized protein.

Impaired formation of mature *nad1* in the *flo22* mutant

It is reported that P-type PPR proteins are mainly involved in processing or stabilizing organelle messenger RNA (mRNA). This led us to hypothesize that the processing of one or more mitochondrial transcripts was defective in the *flo22* mutant. Reverse transcription (RT)-PCR performed to check the transcription level of all mitochondrial protein-coding genes in developing endosperm at 9 DAF showed that transcription level of mature *nad1* containing all exons in *flo22* was drastically reduced compared with the wild type, whereas several mitochondrial genes, including *nad2*, *nad4*, *nad5* were significantly higher (Figure 4A, B). This suggests that a dramatic decrease in the amount of mature *nad1* may cause a compensatory increase in the expression of other ETC components. This phenomenon has also been observed in the *Arabidopsis ppr19* mutant and maize *emp11* mutant (Lee et al., 2017; Ren et al., 2017). To further confirm these results, we designed primers to observe the splicing efficiencies of the 23 introns in mitochondria. RT-quantitative PCR (qPCR) analysis revealed that the splicing efficiencies of *nad1* introns 1 and 4 were reduced more than 30-fold in the *flo22* mutant compared with the wild type and a complemented line (Figure 4C). Splicing of introns 2 and 3 was only slightly affected (Figure 4C), presumably due to splicing defects in introns 1 and 4. These results suggested that FLO22 plays an important role in formation of mature *nad1* transcripts.

Maturation of *nad1* in rice results from the fusion of four mRNA precursors named *nad1* exon 1, *nad1* exon 2-3, *nad1* exon 4, and *nad1* exon 5 (Figure 4D) by three *trans*-splicing events and one *cis*-splicing event (Bonen, 2008). RT-PCR was performed with primers across adjacent exons to find the abnormal splicing events. In the *flo22* mutant, *trans*-spliced transcript exons 1–2 (exon 1 + exon 2) and exons 4–5 (exon 4 + exon 5) were greatly reduced, whereas the level of exon 2–4 (exon 2 + exon 3 + exon 4) was comparable to that of the wild type (Figure 4E). The RT-qPCR experiment verified the above results, and these defects were also rescued in complemented lines (Figure 4F). Notably, the amounts of exon 1–2 and exon 4–5 precursors were drastically reduced in the mutant but only slightly accumulated in the amounts of exon1-intron1a, exon4-intron4a, intron4b-exon5 precursors (Figure 4F). Maturation of exon 2–4 did not appear to be affected. This demonstrated that the defect in the maturation process of *nad1* in the *flo22* mutant was caused by nonsplicing of introns 1 and 4. To corroborate

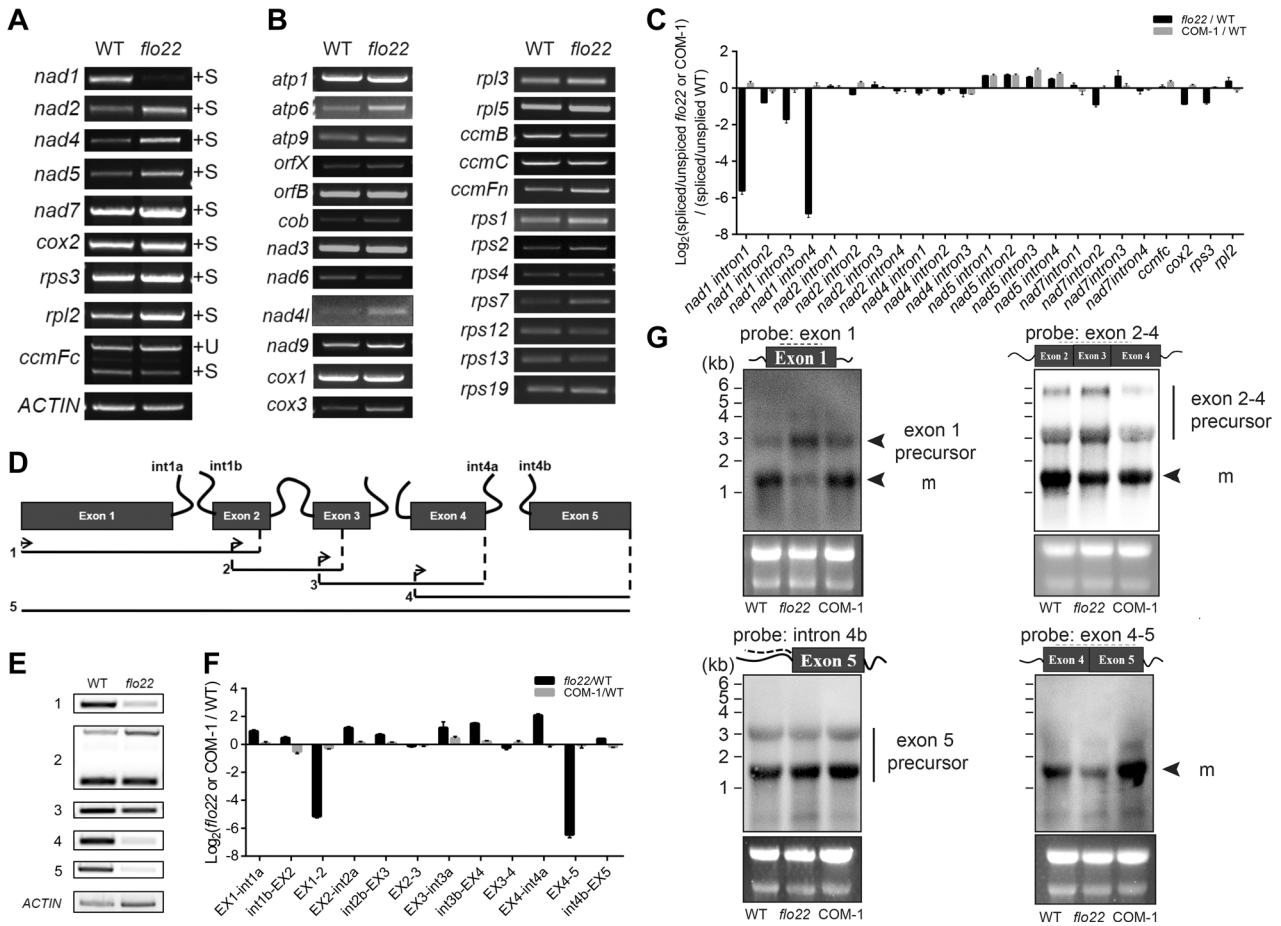

Figure 4. Maturation of mitochondrial *NADH dehydrogenase subunit1 (nad1)* is affected in the *floury endosperm22* (*flo22*) mutant

(**A**, **B**) Reverse transcription – polymerase chain reaction (RT-PCR) analyses of rice mitochondrial intron-containing genes (**A**) and other mitochondrial genes (**B**) in wild type and the *flo22* mutant. *ACTIN* was used as an internal control. +U, unspliced transcripts. +S, spliced transcripts. (**C**) RT-quantitative PCR analyses of all 23 group II introns in mitochondria. Histogram shows the $\log_2$ ratio of spliced to non-spliced RNA in *flo22* mutant or complemented line 1 (COM-1) compared with the corresponding value for the wild type. RNAs were extracted from the wild type, *flo22* mutant and *p35S:FLO22-GFP* complemented grains at 8 d after flowering (DAF). *UBIQUTIN* was used as an internal control. Values are means ± *SD* ($n = 3$). (**D**) Schematic representation of the rice mitochondrial *nad1* gene. Gray boxes indicate exons. Black curved lines indicate introns. The numbers 1–5 and the corresponding straight line show the range of semi-quantitative RT-PCR products. (**E**) RT-PCR results also showing that the splicing events of exon 1–2 and exon 4–5 were affected. (**F**) The deficiencies in splicing events in *flo22* mutant were rescued in complemented lines. The *UBIQUTIN* gene was used as an internal control. Total RNA was extracted from grains at 8 DAF. (**G**) RNA blot analysis confirming the amount of mature *nad1* in the *flo22* mutant was greatly reduced along with a marked accumulation of exon 1 precursors compared to the wild type. The dotted line represents the position of the probe in northern blotting. Staining of ribosomal RNAs with ethidium bromide served as a loading control. RNA size is indicated at the left.

our hypothesis, we conducted an RNA gel blot analysis with probes specifically matching *nad1* exon 1, exon 2–4, intron 4b, and exon 4–5, respectively. The detected amount of mature *nad1* transcripts containing exons 1–2 and 4–5 were significant reduced compared to the wild type and complemented line (Figure 4G). Concurrently, there were slight accumulations of exon1-intron1a precursors in the *flo22* mutant endosperm. However, there was no significant difference in the amount of intron4-exon5 between the *flo22* mutant and the wild type, indicating that splicing of intron 4 might proceed normally (Figure 4G). Combined with the reduction in the amount of mature *nad1* containing exon 4–5 we speculate that the transcript formed after splicing of intron 4 was unstable.

Taken together, all these results indicated that mature *nad1* mRNA is much reduced in the *flo22* mutant probably due to failed splicing of intron 1 and possible instability of mature transcripts.

FLO22 protein binds directly to *nad1* intron 1a

It is widely accepted that each PPR repeat aligns to a base of the target RNA sequence, and that specific recognition is determined by the 5th and 35th amino acids of each motif (Yin et al., 2013; Barkan and Small, 2014; Shen et al., 2016). To better understand the role of FLO22 in the formation of mature *nad1*, we attempted to predict its binding site using a recently published program based on a series of PPR protein-RNA binding experiments (Yan et al., 2019). We obtained degenerate RNA recognition sequences harboring each potential binding site of the FLO22 protein (Figure 5A; Table S2). We then searched the mitochondrial genome for the

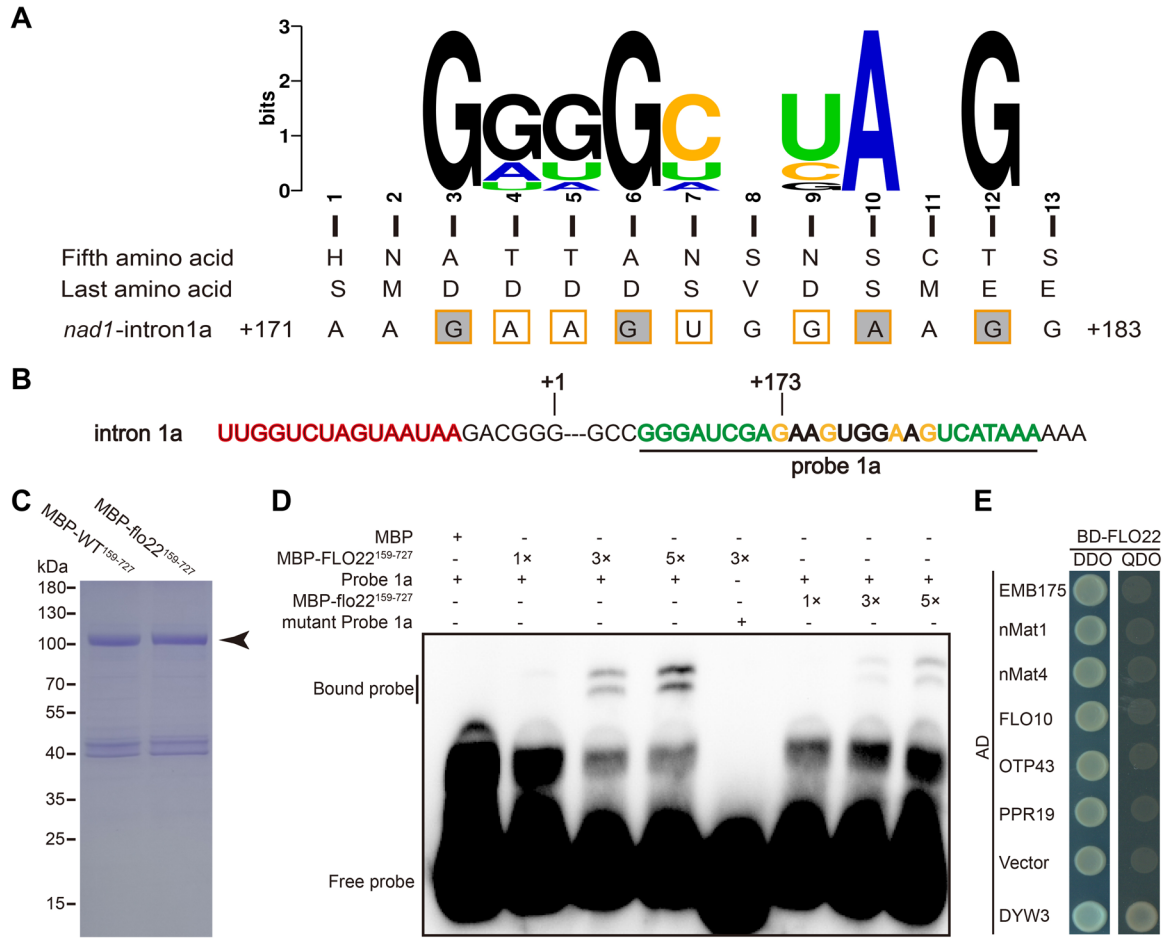

Figure 5. The FLOURY ENDOSPERM22 (FLO22) binding site lies in the region of *NADH dehydrogenase subunit1 (nad1)* intron 1a

(**A**) Prediction of the FLO22 binding site. The sequence logo shows the possible recognition bases and respective probabilities. The fifth and last amino acids of each FLO22 pentatricopeptide repeat (PPR) are listed from N to C termini. We searched the mitochondrial genome for the sequence that best matched the predicted binding sites (Table S3). Combined with the preference of amino acids 5 and 35 for different nucleotides in PPR, we screened out the sequence most likely to be the binding site of the FLO22 in *nad1* intron 1. Orange borders and black shading indicate good matches; only orange borders indicate weaker matches. (**B**) Sequences and position of the probe used in-gel shift reactions. Straight lines indicate the nucleotide sequences of probe 1a. The black nucleotide in the probe is the predicted possible binding site of FLO22, and the green amino acid is the flanking sequence. +1 and +173 indicate the first and 173rd nucleotides after exon 1 of *nad1*. The orange nucleotide sequences indicate the mutation position of the mutant probe 1a, changed to base C, C, U, C, respectively. The red nucleotide sequences represent the exon sequence of *nad1*. (**C**) The purified maltose binding protein (MBP)-FLO22$^{159\text{-}727}$ and MBP-*flo22*$^{159\text{-}727}$ fusion protein were stained with Coomassie Brilliant Blue after polyacrylamide gel electrophoresis. The arrow indicates the fusion protein. (**D**) Electrophoretic mobility shift assay showing binding between MBP-FLO22$^{159\text{-}727}$/MBP-*flo22*$^{159\text{-}727}$ and RNA probes. Proteins were quantified by bicinchoninic acid (BCA) assay. The position of the RNA probes is shown in b. The RNA probe is modified with biotin at the 5' end. (**E**) Yeast two-hybrid assays showing lack of interaction of FLO22 with EMB175 (LOC_Os06g30420), nMat1 (LOC_Os12g21870), nMat4 (LOC_Os06g42770), OTP43 (LOC_Os02g45590), PPR19 (LOC_Os11g04295), and FLO10 (LOC_Os03g07220). The interaction of FLO22 and DYW3 (LOC_Os01g53610) were used as a positive control. DDO represents double dropout supplements (SD/-Leu-Trp) and QDO represents quadruple dropout supplements (SD/-Ade-His-Leu-Trp).

sequence that matched the predicted binding site (Table S3), especially those binding sites at introns 1 or 4. We identified a "GAAGUGGAAG" sequence at 173 bp downstream of exon 1 that was most likely the binding site of FLO22 (Figure 5B). To verify whether FLO22 had a significant affinity for the site, we synthesized a longer RNA probe including the 5' and 3' flanking sequences of the predicted site (Figure 5B) for gel shift assays. A truncated version of wild type and mutant FLO22 lacking its N-terminal 158 amino acids which may include mitochondrial targeting sequence but containing all PPR repeats was expressed in fusion to the maltose binding protein (MBP) in *Escherichia coli* and purified (Figure 5C). Although both wild type and mutant fusion proteins were shown to retard the migration of the *nad1* intron 1a sequence, the binding activity of the mutant protein was significantly weaker than that of the wild type (Figure 5D). Also, the binding between the MBP-FLO22$^{159\text{-}727}$ fusion protein and the mutant sequence was much weaker when the four conserved bases were changed (Figure 5D). All results demonstrated that FLO22 binds specifically to the predicted site *in vitro* and that this binding is significantly weaker when mutation occurs in the *flo22* form. Our results suggested that

FLO22 can directly bind the "GAAGUGGAAG" sequence of intron 1, but we could not find a binding site in intron 4. Numerous PPR proteins are required for *nad1* maturation in different species (Longevialle et al., 2007; Keren et al., 2012; Cohen et al., 2014; Lee et al., 2017; Wu et al., 2019). We speculated that FLO22 functioned in combination with other factor(s) to stabilize *nad1* after removal of intron 4. However, we subsequently found by yeast two-hybrid (Y2H) assay that FLO22 does not directly interact with rice orthologs that control *nad1* intron splicing (Figure 5E).

FLO22 affects complex I activity, respiration rate, and alternative pathways in mitochondria and is important for starch synthesis

NADH dehydrogenase subunit1 (NAD1) are essential members of mitochondria respiratory chain complex I which functions as NAD + hydrogen (NADH) dehydrogenase. Given the deficiency in the maturation of *nad1* transcript, blue native polyacrylamide gel electrophoresis (BN-PAGE) and NADH dehydrogenase activity staining were performed to observe the assembly of complex I and its dehydrogenase activity. As shown in Figure 6A, accumulation of complex I was significantly reduced in the *flo22* mutant compared with the wild type. Staining analyses revealed a dramatic reduction in NADH dehydrogenase activity in the *flo22* mutant (Figure 6A). When the ETC in mitochondria is damaged, plants initiate alternative respiratory pathways that are characterized by up-regulated *AOX* genes. As expected, transcription and translation levels of *AOX* genes were drastically up-regulated in *flo22* mutant endosperm (Figure 6B, C). Transmission electron microscopy of ultrathin sections of developing endosperm at 9 DAF showed that mitochondria in the wild type had densely stacked cristae, whereas mitochondria in the *flo22* mutant had unshapely cristae with large internal spaces (Figure 6D). The function and morphology of the mitochondria in complemented line 1 were restored to those in the wild type (Figure 6A–D). These results indicated that the disrupted RNA processing in *flo22* mutant endosperm affected the assembly and activity of complex I and development of mitochondria.

Mitochondria as "energy factories" provide ATP for metabolism. High-throughput RNA sequencing conducted to determine the consequences of abnormal mitochondrial morphology and function identified 1,473 down-regulated genes and 1,963 up-regulated genes in the *flo22* mutant compared to the wild type. Kyoto Encyclopedia of Genes and Genomes (KEGG) pathway enrichment analysis showed that the differentially expressed genes (DEGs) were involved in various processes (Datasets S2–S4; Figure S4A, B). DEGs participating in the tricarboxylic acid (TCA) cycle and oxidative phosphorylation were highly up-regulated in mutant endosperm, whereas the DEGs involved in plant hormone signal transduction and starch and sucrose metabolism were significantly down-regulated (Figure S4A–D). Expression levels of multiple auxin-responsive genes, such as *IAA6, 10, 14, 21, 23, ARF2*, and *Auxin transporter-like protein 1* (*LAX1*), were significantly down-regulated in the mutant. Expression of starch synthesis-related genes were also lower in the mutant (Figure S4E). Transcripts of *AGPL1* and *AGPS1*, the two genes coding for subunits of the first key rate-limiting enzyme AGPase in endosperm starch synthesis, were significantly reduced in the *flo22* mutant (Figure S4C), whereas expression levels of genes related to oxidative phosphorylation and the TCA cycle pathway that supplies energy were significantly increased (Figure S4D). This was confirmed by RT-qPCR analysis of several selected representative genes (Figure S4F, G).

Mitochondria play essential roles throughout the entire life cycle of plants. To determine the effect of the mutation on plant growth we investigated the membrane potential of mitochondria and respiration rates of seedlings. Compared with the wild type and the complemented line 1, the membrane potential mitochondria in the mutant were decreased by 50% (Figure 6E) and respiration rate was reduced by 15% (Figure 6F).

Together, the disrupted function of FLO22 affected the assembly and activity of complex I, and RNA-seq assays indicated a severe effect on mitochondrial oxidative phosphorylation and other cellular activities like starch and sucrose metabolism in the *flo22* mutant.

Editing efficiencies of multiple mitochondrial edited sites are altered in the *flo22* mutant

FLO22 is an atypical P-type PPR protein. Most of its motifs are 35-amino acid P motifs, but also contain two S motifs (Figure 2B). To date, the vast majority of the research on P-type PPR protein has focused on splicing and stabilization of organelle RNAs. However, studies by Andres-Colas et al. (2017) and Guillaumot et al. (2017) revealed the presence of PPR editosomes in which P-type PPR protein assists interaction between DYW-type PPR protein DYW2 and E^+-type PPR protein SLO2 or CLB19 in *Arabidopsis*. The three different types of PPR proteins form a complex possessing both RNA sequence targeting and C-to-U editing functions that are responsible for multi-site editing of mitochondrial and chloroplast mRNAs. To determine whether FLO22 was involved in the organelle RNA editing in rice, we determined the editing efficiencies of RT-PCR products covering all known mitochondrial editing sites. The editing efficiencies of tens of editing sites were changed; most sites were down-regulated but several were up-regulated (Table S4). In particular, the editing efficiencies of multiple sites of mitochondrial *nad9* mRNA were decreased by 30% and resulted in the alternation of amino acids. Meanwhile, the editing efficiencies of these sites in complemented line 1 were comparable to those of the wild type (Figure 7A). In contrast, the editing efficiencies of the three sites of *nad1* and *nad7* mRNA were slightly up-regulated in *flo22* (Table S4). Overall, the editing efficiencies of multiple mitochondrially edited sites were altered in *flo22* mutant endosperm, and obviously the largely changed sites concentrated on the members of respiratory chain complex I.

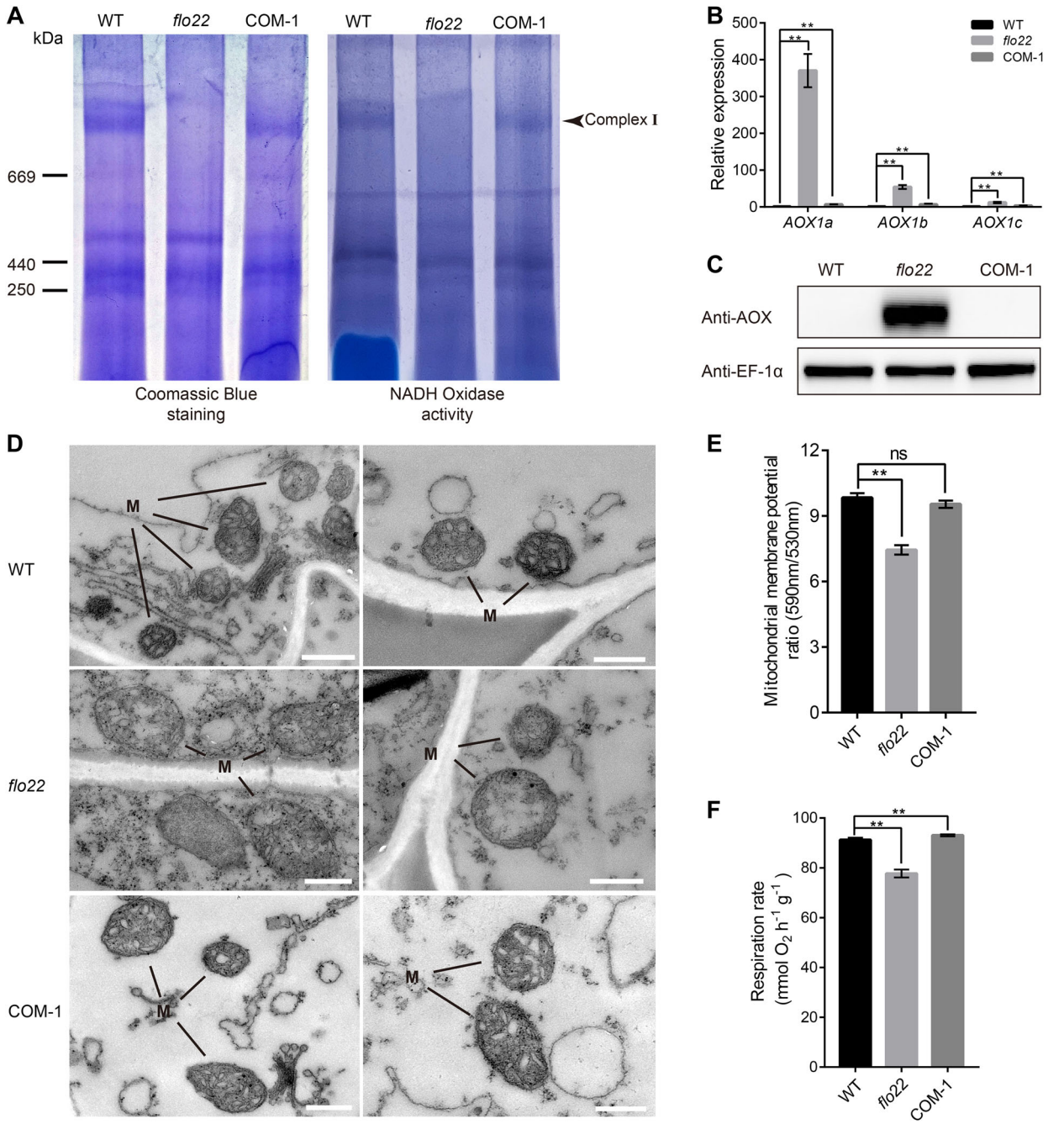

Figure 6. Mutation of *FLOURY ENDOSPERM22* (*FLO22*) affects nicotinamide adenine dinucleotide + hydrogen (NADH) dehydrogenase activity and mitochondrial morphology and function

(**A**) Complex I assembly and activity analyses in wild type, *flo22* mutant and complemented line 1. Left, Coomassie Brilliant Blue staining of mitochondrial complexes separated by blue native polyacrylamide gel electrophoresis (BN-PAGE). Right, in-gel NADH dehydrogenase activity staining for complex I. (**B**) Transcript levels of alternative oxidases (*AOX1a*–*c*) in 9 d after flowering (DAF) endosperm of *flo22* and complemented line 1 relative to the wild type level. Rice *UBIQUTIN* gene was used as an internal control. Values are means ± *SD* ($n = 3$). (**C**) Total proteins extracted from 9 DAF endosperm were detected with AOX antibodies. Anti-EF-1α antibodies were used as a loading control. (**D**) Transmission electron microscopic images of mitochondria in wild type, *flo22* mutant and complemented line 1 endosperm at 9 DAF. M, mitochondria. Bar, 500 nm. Measurement of mitochondrial membrane potential (**E**) and respiration rate (**F**) of wild type, *flo22* mutant and complemented line 1. Ns, not significant. Values are means ± *SD* from three biological replicates. Student's *t*-tests (**$P < 0.01$).

Although P-type PPR proteins have been previously reported to play a role in enhancing the interactions of various editing factors (Andres-Colas et al., 2017; Guillaumot et al., 2017; Wang et al., 2022; Yang et al., 2022), we tried to find potential binding sites for FLO22 on *nad9* due to its large number of sites with reduced RNA editing efficiency in *flo22*. Four of the six most likely FLO22 binding sites masked the editing site or were less than five bases away from the editing

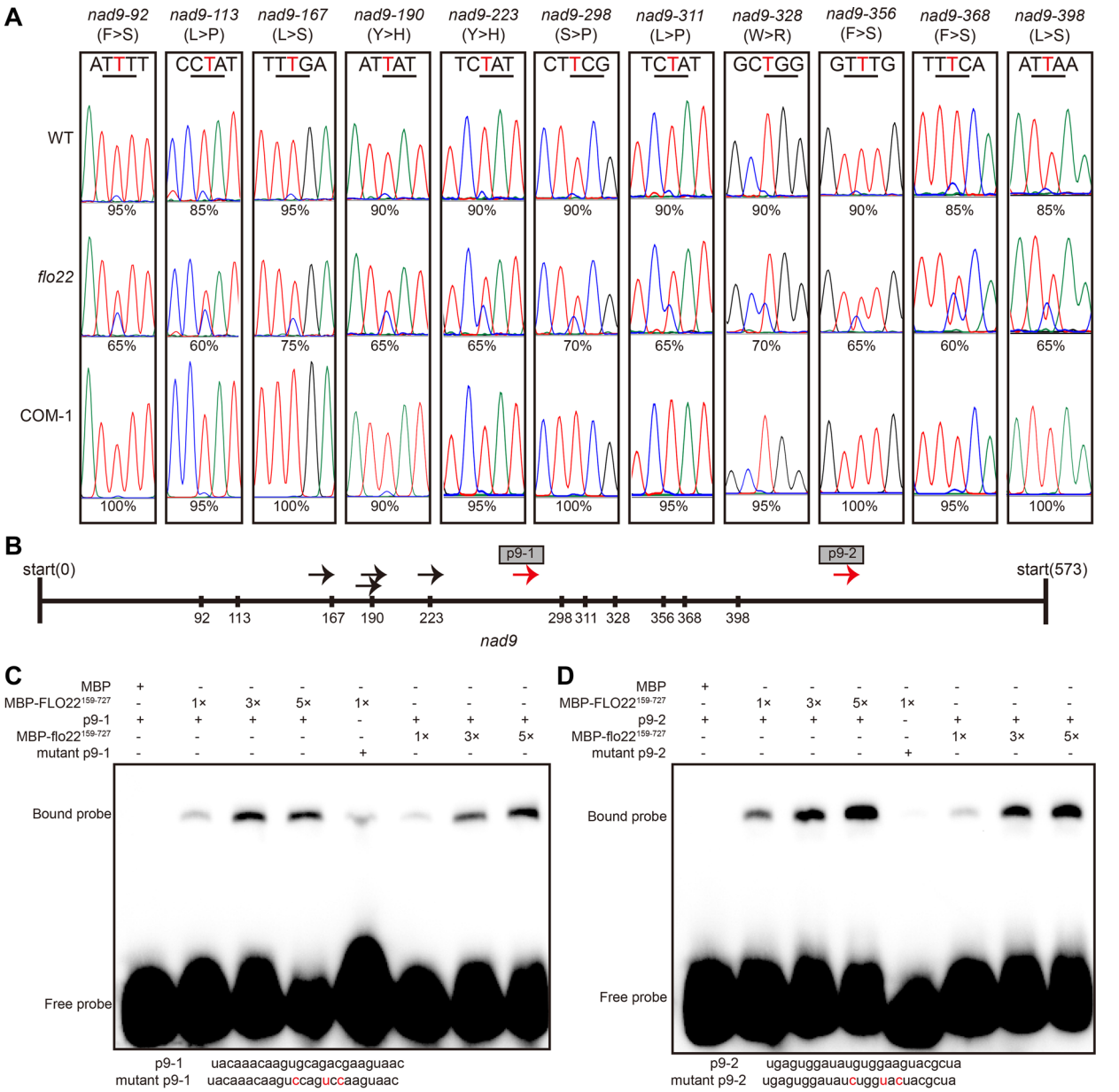

Figure 7. Editing efficiencies of multiple edited sites in *NADH dehydrogenase subunit9* (*nad9*) were altered in the *floury endosperm22* (*flo22*) mutant

(**A**) Sequence analysis of reverse transcription – polymerase chain reaction (RT-PCR) productions showing that multiple editing events in *nad9* were largely affected. Total RNAs extracted from grains of wild type, *flo22* mutant and complemented line 1 at 8 d after flowering (DAF) were subsequently reverse-transcribed. Using primers covering the mitochondrial editing sites, we performed PCR amplification and sequencing. Sequencing results revealed tens of affected editing sites, mainly down-regulated, but also including several up-regulated sites (Table S4). In particular, the editing efficiencies of multiple sites of mitochondrial *nad9* messenger RNA were decreased by 30% and resulted in the alternation of amino acids. The editing sites are listed at the top. The changes in amino acids caused by editing and non-edited events are shown in parentheses. Sequencing chromatograms are displayed. Codons containing the editing sites are underlined, and edited sites are marked in red. The RNA editing efficiencies are shown below the sequencing chromatograms. (**B**) Prediction of possible binding sites for FLO22 on *nad9* transcript. The numbers show the position of editing sites. The arrows indicate the position of the most matched nucleotide sequences, and the red marked arrows indicate the position of the two potential binding sites that we designed for the corresponding probes (p9-1, p9-2) for further *in vitro* binding experiments. (**C**, **D**) Electrophoretic mobility shift assay showing binding between maltose binding protein (MBP)-FLO22$^{159\text{-}727}$/MBP-*flo22*$^{159\text{-}727}$ and RNA probes. Proteins were quantified by bicinchoninic acid (BCA) assay. The probe sequences are listed at the bottom of the graph, and the positions of the mutated bases are marked in red.

site (Figure 7B; Table S5). Electrophoretic mobility shift assay (EMSA) confirmed that FLO22 could bind to the remaining two nucleotide sequences p9-1 and p9-2 on *nad9* (Figure 7C, D). The mutant protein binds significantly weaker to p9-2 compared with wild type protein, while it does not change much with p9-1 (Figure 7C, D). Meanwhile, the recognition of the mutated p9-1 sequence by FLO22 was not significantly weaker when three conserved sites were changed (Figure 7C).

However, the site where FLO22 binds *nad9* is clearly distant from these editing sites (Figure 7B), implying that FLO22 may have a different role in the editing process than conventional PLS-type PPR proteins.

FLO22 and DYW3 proteins cooperate in mitochondrial RNA editing

The process of RNA editing includes recognition of target sequences and deamination of cytidine. Hypothetically, the PPR protein editing complex consists of DYW-type PPR proteins and provide editing catalytic domains and PLS-type PPR proteins that target specific RNA sites. This means that FLO22 might associate with DYW-type and PLS-type PPR proteins to complete editing events. To verify this hypothesis, we obtained a summary of 457 PPR protein-encoded genes from the crop and model plant genome information database Gramene (http://www.gramene.org/) and divided them into three categories, namely, P-type, DYW-type, and PLS-type without a DYW domain (Dataset S1). We further found 6 DYW-type PPR proteins with less than 6 PPR repeats. Moreover, due to the mitochondrial localization of FLO22 we cloned 37 PLS-type proteins without a DYW domain and possibly mitochondrially localized as predicted by TargetP (Dataset S1). Y2H and bimolecular fluorescence complementation (BiFC) assays were performed to determine whether FLO22 interacted with DYW-type PPR protein DYW3, and PLS-type PPR proteins PLS31 and PLS33 (Figures 8A–C, S5A, B). As shown in Figures 8C and S5B, yellow fluorescent protein (YFP) signals were detected when FLO22 was combined with the other three PPR proteins. Colocalization of YFP signal and OsCOX11-mCherry (Han et al., 2021) suggested that these interactions took place in mitochondria (Figures 8C, S4B). It is acknowledged that BiFC assays also detect the weak and transient interactions. Pull-down assays performed using MBP-FLO22 fusion protein in combination with the other three His-tagged PPR proteins showed that only DYW3 strongly interacted with FLO22 *in vitro* (Figure 8D).

We attempted to knockout DYW3 in a *japonica* variety Ninggeng 7 (NG7) to further verify whether the altered editing efficiency in the *flo22* mutant was caused by the abnormal PPR complex. One homozygous single base insertion T_0 mutant and several heterozygous mutants were obtained (Figure S6A). We then assessed the mitochondrial mRNA editing efficiency of the homozygous T_0 mutant *#34* and heterozygous T_0 mutants *#38* and *#29* with deletions of 4/15 and 21/42 bases, respectively (Figure S6B, C). Surprisingly, instead of *nad9*, the editing efficiencies of sites *nad2-853*,

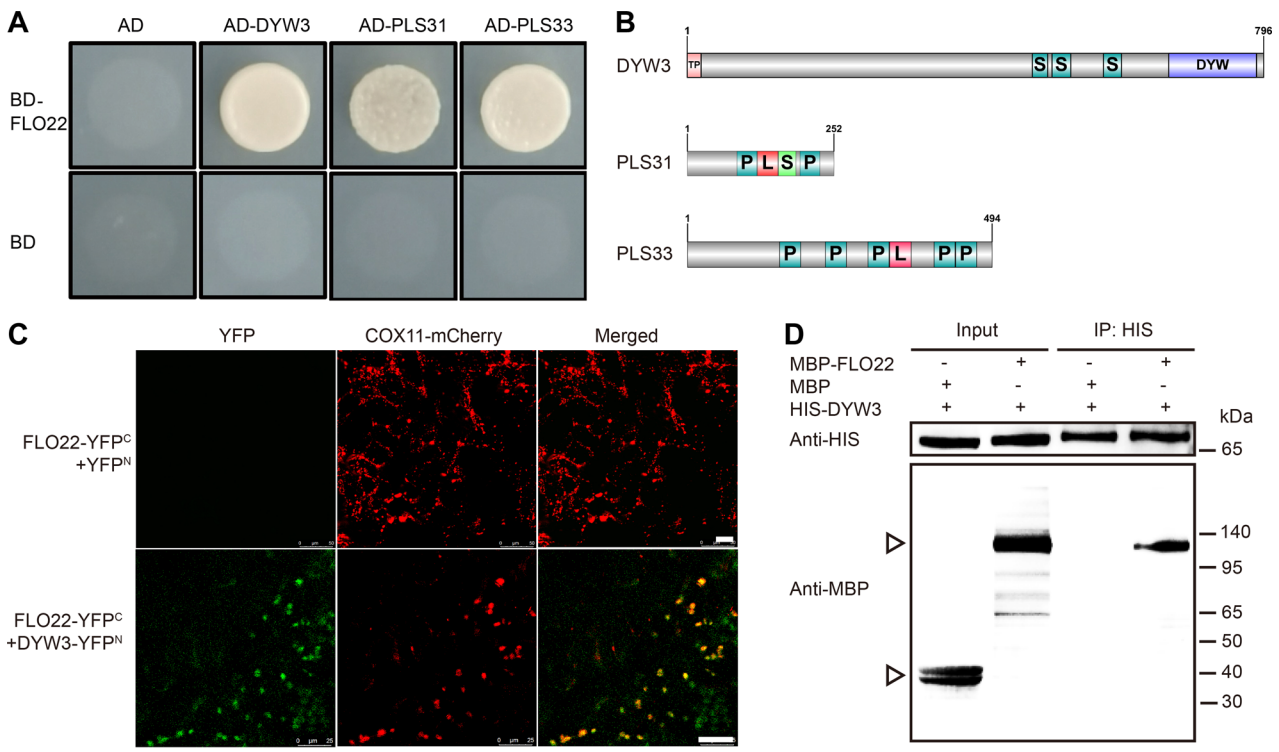

Figure 8. FLOURY ENDOSPERM22 (FLO22) and DYW3 proteins interact in mitochondria

(**A**) Yeast two-hybrid assays showing that FLO22 interacts with DYW3 (*LOC_Os01g53610*), PLS31 (*LOC_Os10g35440*) and PLS33 (*Os01g0913800*). (**B**) Schematics of the three pentatricopeptide repeat (PPR) proteins interacting with FLO22. P, PPR with 35 amino acids; L, long PPR with 36 amino acids; S, short PPR with 31 amino acids; TP, transit peptide. (**C**) Bimolecular fluorescence complementation (BiFC) assays showing that FLO22 interacts with DYW3; the yellow fluorescent protein overlaps with COX11-mCherry localized in mitochondria. Bars, 25 μm. (**D**) *In vitro* pull-down assay indicates that recombinant maltose binding protein (MBP)-FLO22 protein strongly interacts with recombinant His-DYW3 protein. Arrows indicate MBP and MBP-fusion proteins. Numbers on the right indicate the protein size. kDa, kilodaltons.

nad3-362, and *nad4-6065* were slightly affected and led to amino acid changes (Figure S6B). Although the C-to-U alteration at *nad1-537* and *ccmFn-37* were affected, the two editing events did not affect the final amino acid sequence (Figure S6C). We previously found that the editing efficiency of *nad1-537* was increased by two-fold in the *flo22* mutant compared with the wild type. This overlapping site suggests that FLO22 and DYW3 may function in the same complex. Considering the complexity of the plant editing system (Small et al., 2020), we speculate that the role of DYW3 was replaced in the *DYW3* knockdown mutants by other DYW-type PPR proteins or unknown factors with deaminase activity. This compensation effect may cause editing deficiencies at other sites.

To determine whether DYW3 plays a similar biological function to FLO22, we observed plant growth and endosperm development in the DYW3 mutants. Plant *#34* with deletion of a single nucleotide had severely affected plant growth and development and produced no seeds (Figure S6D). We obtained seeds with deletions of 3, 6, 15, and 21/42 bases, which ultimately resulted in deletions of one to 13 amino acids (Figure S6E, F). The seeds of the homozygous 15 bp deletion and the heterozygous 21/42 bp deletion exhibited opaque phenotypes, but the homozygous 3 and 6 bp deletion mutants had normal appearance (Figure S6E). It is possible that the deletion of large fragments may affect the secondary structure of the DYW3 protein, which in turn affects the function of the protein (Figure S6E, F).

Therefore, knockdown of DYW3 also affecting plant growth and endosperm development suggested that FLO22 might act synergistically with DYW3 in mitochondrial editing events.

DISCUSSION

FLO22 is important for mitochondrial function and endosperm development

Here we showed that mutation of FLO22 significantly affected RNA processing of mitochondrial genes *nad1* and *nad9*. NADH dehydrogenase, the core component of ETCs, consists of nine subunits, including NAD1-4, NAD4L, NAD5-7, and NAD9 (Braun et al., 2014). We believe that the substantial reduction in mature *nad1* transcript in the mutant most likely caused the defects in mitochondrial function and morphology of the *flo22* mutant (Figure 6A–F). These defects, which directly affect mitochondria as an energy source, obviously had impacts on the entire life cycle of the mutant (Figure 1A–L), a phenomenon common to all PPR protein mutants (Yang et al., 2017; Sun et al., 2018; Xiao et al., 2018; Hao et al., 2019; Wang et al., 2019; Wu et al., 2019). The *Arabidopsis ppr19* mutant displays a lack of mitochondrial complex I and retarded growth phenotype (Lee et al., 2017). In maize, *emp10*, *emp11*, and *dek2* mutant show impaired plant growth and lethal embryos (Cai et al., 2017; Qi et al., 2017; Ren et al., 2017), and the endosperm development of rice *flo10* and *fgr1* mutants is also affected (Hao et al., 2019; Wu et al., 2019).

KEGG analysis of RNA-seq data indicated that many cellular processes are disrupted in *flo22* mutant endosperm (Dataset S4; Figure S4A–D). In particular, AGPS1 and AGPL1, as components of the key rate-limiting enzyme AGPase in starch synthesis, need to consume ATP to generate ADPG, which in turn initiates starch synthesis (Dataset S4; Figure S6C, E). Substantial downregulation of these two genes led us to believe that energy deficiency was the main cause of defective starch synthesis in the *flo22* mutant. Upregulation of TCA cycle, oxidative phosphorylation and carbohydrate metabolic pathway genes were likely feedback responses to abnormal ETCs (Figure S4D). Taken together, mitochondrial dysfunction caused by abnormal RNA processing in the *flo22* mutant was responsible for slow starch accumulation in endosperm cells, delayed development of amyloplasts and impaired plant growth.

FLO22 is required for processing of mature *nad1*

P-type PPR proteins are mainly invovled in the splicing of group II introns in plant mitochondrial and plastid genome, which is essential for organelle mRNA maturation (Cai et al., 2011; Chen et al., 2017; Wang et al., 2017; Wu et al., 2019). For example, ZmDEK2 is responsible for the *trans*-splicing of mitochondria *nad1* intron 1, and AtPPR19 and ZmEMP11 regulate the splicing of all *nad1* introns (Lee et al., 2017; Qi et al., 2017; Ren et al., 2017; Wang et al., 2017). In rice, FLO10, a mitochondrially localized P-type PPR protein, was associated with processing of *nad1* exon 1 precursors (Wu et al., 2019).

Splicing efficiency analysis and RNA gel assays in this study indicated that the abundance of mature *nad1* in the *flo22* mutant was drastically reduced and that ex1-int1a and exon 2–4 precursor slightly accumulated in *flo22* (Figure 4E, F). This appears to be similar to defects observed in a *flo10* mutant (Wu et al., 2019), suggesting important roles for both wild type alleles in splicing of intron 1. RNA-EMSA assays indicated that FLO22 bound to the sequences in the 3' untranslated region of exon 1, suggesting that it directly participates in the processing of ex1-int1a precursor (Figure 5A–D). Although the FLO22 protein levels were slightly increased in the mutant compared to that in the wild type (Figure 2D), we believe that the weakened binding activity of the *flo22* mutant protein with intron 1a is responsible for the defective splicing of *nad1* intron 1 (Figure 5D). The int4-ex5 precursor did not accumulate significantly, but the amount of mature *nad1* containing ex4-5 also decreased sharply, suggesting that the stability of *nad1* after intron 4 splicing in the *flo22* mutant may be affected. However, it is not yet clear whether FLO22 participates in stabilizing ex4-5 since no binding site was identified. In *Arabidopsis*, maize and rice multiple P-type PPRs are important for the splicing of the same introns (Keren et al., 2012; Cohen et al., 2014; Lee et al., 2017; Wu et al., 2019). Diverse RNA-binding proteins and editing factors combine to function in the form of editosomes (Sun et al., 2016). Therefore, it is also likely that PPR proteins form a

splicing complex. Although we did not find direct interaction between FLO22 and rice orthologous proteins of genes reported to be involved in *nad1* maturation, including FLO10 (Figure 5E), the possibility of a splicing complex cannot be ruled out.

FLO22 functions in the editing complex

PPR proteins reported for editing plastid and mitochondrial transcripts during the past 30 years almost all belong to the PLS subfamily (Cai et al., 2009; Kim et al., 2009; Toda et al., 2012; Li et al., 2014; Brehme et al., 2015; Yang et al., 2017). Among them, some PLS-type PPR proteins are responsible for multiple editing sites and do not have DYW domains (Zhu et al., 2012; Yang et al., 2017). This means that they may play a role of targeting in editing events while other proteins carry out deamination processes. Furthermore, mitochondrial and chloroplast genomes of land plants have many hundreds of editing sites (Sun et al., 2016) and most of the nuclear-encoded PPR proteins are P-type (Dataset S1; Fujii and Small, 2011; Barkan and Small, 2014; Sun et al., 2016). The PLS-type, especially DYW-type, PPR proteins obviously cannot satisfy one-to-one editing events at a single site. Therefore, it is plausible that various PPR proteins form editing complexes to perform their functions. A PPR editing complex first proposed in *Arabidopsis* suggested that E^+-type PPR proteins target specific RNA sites and P-type PPR protein NUWA assisted the interaction between the E^+ partner and DYW2 (Andres-Colas et al., 2017; Guillaumot et al., 2017). *Arabidopsis* GRP23 and maize BCCP1 have similar roles in the editing complex (Wang et al., 2022; Yang et al., 2022). To date, there are no further reports of other PPR editing complexes in rice.

We found that all 11 sites with >30% decline in the *flo22* mutant were in *nad9* transcripts, but a significant portion of correctly edited sites still existed (Figure 7A). It is unknown whether the non-corrected sites affect the stability of NAD9 and whether they affect the assembly of complex I (Figure 6A). At the same time, cytidines at the *nad1-537*, *nad7-99*, and *nad7-2438* sites were edited more frequently, and editing efficiency of *nad1-537* in particular was much improved. Similar phenomena were observed in the maize *emp5* (Liu et al., 2013) and *Arabidopsis slo2* (Zhu et al., 2012) mutants. It seems that PPR editing factors work on overlapping sites and a functional defect of one PPR protein may cause compensatory expression of other editing factors at the same site.

Based on previous studies we screened out one DYW-type DYW3 protein and two PLS-type proteins (PLS31 and PLS33) which directly interact with FLO22 (Figure 8A). The interaction between FLO22 and DYW3 seemed more stable according to the BiFC and pull-down assays, but interaction between FLO22 and the other two PLS-type PPR proteins was observed at very low frequencies. DYW3 contains three PLS repeats and one additional DYW domain harboring a conserved HxExnCxxC motif that is similar to the active-site of cytidine deaminase (Figure 8B). Fewer PLS repeats suggest that DYW3 might be unable to accurately locate the target sequence and the DYW domain could provide deaminase function. DYW3 is also essential for seed development. We were not able to harvest seeds from one mutant with a frameshift mutation, and deletion of some large segments of DYW3 also affected grain filling, resulting in partially opaque phenotypes (Figure S6E). Therefore, we assumed that FLO22 and DYW3 work synergistically in a PPR complex to perform editing events. On the other hand, PLS31 and PLS33 contain only four and six PLS repeats, respectively (Figure 8B). We are not sure that these two PPR proteins have the role of locating editing sites in the complex. Hence, there is a possibility that other factor(s), maybe E^+-type PPR protein(s), recognize target sequences in the complex. In addition, FLO22 can also bind the *nad9* transcript (Figure 7C, D). Recently, the P-type PPR proteins AtNUWA, AtGRP23 and ZmBCCP1 have been reported playing a role in the complex of enhancing the interaction between editing factors in both *Arabidopsis* and maize (Andres-Colas et al., 2017; Guillaumot et al., 2017; Wang et al., 2022; Yang et al., 2022). Combined with the above, due to multiple change sites observed in *nad9* of the mutant and the fact that the target sequence of *nad9* bound by FLO22 is far from these sites (Figure 7B, D), we speculate that the FLO22-RNA binding in the complex may be intended to ensure overall stability between editosome and transcripts for efficient editing process.

RNA editing in plant organelles requires participation of various proteins that can form complexes to ensure editing events (Fujii and Small, 2011; Sun et al., 2016; Small et al., 2020). Our study revealed that FLO22 not only regulates the maturation of *nad1* transcripts but also can participate in multi-site RNA editing together with DYW3, which is essential for normal mitochondrial function and further overall plant growth and endosperm starch synthesis (Figure S7). For the first time, we propose that multiple types of PPR proteins jointly participate in RNA editing in rice mitochondria and will continue to explore the role of complexes in endosperm development.

MATERIALS AND METHODS

Plant materials and growth conditions

The *flo22* mutant was isolated from an MNU-treated population of the *indica* variety N22. All plants were grown in natural and well-managed paddy fields or plant growth chambers (12 h light/12 h darkness at 28°C). Endosperm at 6-18 DAF and other tissues such as roots, panicles, stems, leaves, and leaf sheaths were collected and immediately used for experiments or stored at −80°C.

Microscopy

Mature seeds were prepared as described (Peng et al., 2014) and observed by SEM (HITACHI, S–3400 N). Ultrathin and semithin sections of endosperm of 9 DAF were cut into slices (~2 mm) and fixed before embedding and staining as previously described (Peng et al., 2014; Wu et al., 2019). Semithin sections (1 μm) were stained with iodine-potassium iodide (I2-KI) and observed under a light microscope (80i, Nikon). Samples for

transmission electron microscopy were cut into 50 to 70 nm sections and observed with a Hitachi H-7650 microscope.

Measurement of total starch, amylose and lipid contents

Total starch contents of mature seeds from N22 and the *flo22* mutant were measured with an assay kit, following the manufacturer's instruction (Megazyme). Amylose and lipid contents were determined following a method previously mentioned (Hao et al., 2019).

Map-based cloning and genetic complementation

To map the *FLO22* locus, the mutant was crossed with *japonica* cultivar Ninggeng 4 (NG4). For initial mapping, 10 floury individuals were selected from the F_2 population. The *FLO22* locus was then fine mapped to a region of ~170 kb with 1,000 individuals. All markers used for positional cloning are shown in Table S1. To verify the candidate gene, the coding sequence of *LOC_Os07g08180* was amplified and cloned into the pCAMBIA1300-221-3*flag binary vector. The construct was then introduced into *Agrobacterium tumefaciens* (strain EHA105) for transformation of *flo22* calli.

Subcellular localization analysis

For transient expression analysis the coding sequence of *LOC_Os07g08180* was separately cloned into pCAMBIA1305GFP and pAN580GFP under the control of the CaMV35S promotor. The pCAMBIA1305-FLO22-GFP fusion construct was introduced into *A. tumefaciens* strain EHA105 and then used to infect the *Nicotiana benthamiana* leaves. The pAN580-FLO22-GFP fusion construct was transformed into rice protoplasts and incubated in darkness for 16 h at 28°C. Mito-Tracker Orange CM-H2TMRos (0.5 mmol/L; Invitrogen) was injected into *N. Benthamian* leaves or added to protoplast suspensions for 30 min to dye the mitochondria. Observations of subcellular localization were made with a confocal laser scanning microscope (Leica, SP8).

RNA extraction, RT-PCR and RT-qPCR analysis

Total RNA from endosperm at 8 DAF and other tissues were isolated and reverse-transcribed as described before (Hao et al., 2019). RT-qPCR was performed using an ABI 7500 Real-Time PCR system and the rice *UBIQUITIN* gene was used as the internal control. Semi-quantitative PCR was performed to visualize the abundance of mitochondrial genes and splicing of *nad1*. The rice *ACTIN* gene was used as the internal control. All the primers used in RT-PCR and RT-qPCR were from Wu et al. (2019).

Northern blotting

Probe template was PCR amplified with primers listed in Table S1. The probe was labeled with a DIG Northern Starter Kit (Roche) following the manufacturer's instructions. Total RNA was extracted from 8 DAF endosperm and then hybridized with the probe as described (Wu et al., 2019).

Prediction of the RNA binding site of FLO22

The fifth and last amino acid of the P-type motif determines the possible RNA binding sequence. Using the website (http://yinlab.hzau.edu.cn/pprcode/) developed by Yan et al. (2019) we predicted target RNA bases to which each motif of FLO22 might bind and the corresponding probability (Table S2).

Purification of the recombinant FLO22 protein and RNA binding assay

The *FLO22/flo22* coding sequence deprived of upstream 474 nucleotides were cloned into the pMAL-c2X vector to produce the recombinant proteins with an N-terminal MBP-tag. The recombinant protein was purified as previously described (Hao et al., 2019). The purified proteins were quantified by bicinchoninic acid (BCA) assay using Pierce™ BCA Protein Assay Kit. Probes were synthesized with biotin at the 5'-terminal (Genscript, Nanjing). Analysis of MBP-FLO22 and RNA binding was performed using a Thermo Fisher LightShift™ Chemiluminescent RNA EMSA Kit (No. 20158) following the manufacturer's instructions.

BN-PAGE and activity staining of NADH dehydrogenase

Crude mitochondria were isolated from 10-d-old seedling as previously described (Wang et al., 2017). Twenty microliters of protein samples were loaded onto 3%-12% gradient polyacrylamide gels for electrophoresis as previously described (Wu et al., 2019). Gels for NADH complex I activity analysis were either stained with Coomassie Brilliant Blue R-250 or incubated in detection buffer (50 mmol/L MOPS-KOH, pH 7.6, 1 mmol/L Nitro blue tetrazolium and 0.2 mmol/L NADH).

Protein extraction and immunoblot analysis

Total proteins were isolated from grains at 9 DAF and subjected to gel electrophoresis as previously described (Wu et al., 2019). The protein was transferred to a polyvinylidene fluoride membrane and incubated with polyclonal antibodies against alternative oxidase (AOX) (Agrisera, AS04054), polyclonal antibodies against FLO22 and polyclonal antibodies against EF-1α. Polyclonal antibodies of FLO22 were raised against the peptide CIRVWEEIRRDHVDP in rabbits. Antibodies were antigen affinity-purified from the immune serum. Goat anti-mouse and goat anti-rabbit (1:2,000 dilution) were used as the secondary antibodies.

Measurement of mitochondrial membrane potential and respiration rate

Protoplasts were isolated from 9-d-old seedlings grown in darkness. Mitochondrial membrane potential was measured using a JC-1 kit (Beyotime, China) following the manufacturer's instructions.

Total respiration rate was measured by a liquid-phase oxygen electrode (Hansatech, UK) using seedlings of the wild type and mutant grown in darkness.

Analysis of mitochondrial RNA editing

Total RNAs for RNA editing analysis were isolated from endosperm at 9 DAF or seedlings and reverse-transcribed as above. Primers covering the mitochondrial editing sites were synthesized for RT-PCR following previous reports (Robbins et al., 2009; Zhang et al., 2017). RNA editing efficiencies were measured by the proportion of height of the "T" nucleotide accounting for the sum of "T" and "C" nucleotides. This analysis was performed with three biological replicates.

Y2H assays

The coding sequence of *FLO22* was PCR amplified and cloned into pGBKT7 and other potential interaction factors were cloned into pGADT7 (Clontech). Both types of constructs were respectively co-transformed into the yeast strain AH109. Yeast transformation and screening procedures were performed according to the manufacturer's instructions (Clontech). The gene information of PPR proteins is shown in Dataset S1.

BiFC assay

The coding sequence of *FLO22* was cloned into the binary vector pSPYCE(M) to create pFLO22-YFP^{C}. Full-length complementary DNAs (cDNAs) of *DYW3*, *PLS31*, and *PLS33* were cloned into the binary vector pSPYNE173 to produce recombinants harboring the N-terminus of YFP protein. The plasmids were transformed into *A. tumefaciens* (strain EHA105), and then infiltrated into tobacco leaves as previously described (Waadt and Kudla, 2008). A confocal laser scanning microscope (Leica, SP8) was used for fluorescence detection.

In vitro pull-down assay

Recombinant protein MBP-FLO22 was prepared as described above. For *in vitro* pull-down experiments full-length *DYW3*, *PLS31*, and *PLS33* cDNAs were cloned into the pET30a vector to produce His-tag fused proteins. The constructs were introduced into *E. coli* (BL21). The supernatants of His-tag fused proteins were initially loaded onto His resin. After incubation for 2 h at 4°C, the resins were washed three times using wash buffer (50 mmol/L NaH_2PO_4, 300 mmol/L NaCl, 10 mmol/L imidazole pH 8.0). The supernatant of MBP-FLO22 was then loaded onto His-DYW3/PLS31/PLS33 binding resin and MBP protein was used as a negative control. The resins were again washed up to three times after incubation before being finally boiled in sodium dodecyl sulfate (SDS)-PAGE buffer for 5 min at 95°C. The eluted proteins were detected using monoclonal antibodies against His-tag (Millipore, dilution 1:5,000) and MBP-tag (New England Biolabs, dilution 1:5,000), respectively.

RNA-seq

Total RNAs were isolated from grains at 9 DAF in three biological replicates per sample using Trizol reagent followed by sequencing on a HiSeqTM instrument (Illumina). After filtering, about 6 Gb of clean bases were obtained per sample. The filtered reads were then mapped to the rice reference genome (MSU7.0). DEGs were filtered for $|\log_2(\text{FoldChange})| > 1$ and adjusted P (q-value) <0.05 (Dataset S2). Gene Ontology (GO) and KEGG analyses were performed using AgriGo and RStudio (Datasets S3, 4).

ACKNOWLEDGEMENTS

This work was supported by grants from the National Key R&D Program of China (2021YFF1000200), National Natural Science Foundation of China (31901513), the "JBGS" Project of Seed Industry Revitalization in Jiangsu Province (JBGS [2021]008), Jiangsu Province Agriculture Independent Innovation Fund Project (CX(19)1002), the Fundamental Research Funds for the Central Universities (KJQN202005) and the China Postdoctoral Science Foundation (2019M661864). This work was also supported by the Key Laboratory of Biology, Genetics, and Breeding of Japonica Rice in Mid-lower Yangtze River, Ministry of Agriculture, China, the Jiangsu Collaborative Innovation Center for Modern Crop Production, and National Observation and Research Station of Rice Germplasm Resources, Nanjing, Jiangsu.

CONFLICTS OF INTEREST

The authors declare no conflicts of interest.

AUTHOR CONTRIBUTIONS

J.M.W. and Y.H.W. planed and designed the experiments; H. Y., Y.L.W. and Y.L.T. performed most of the experiments, and H.Y. wrote the manuscript; Y.L.W. and Y.H.W. analyzed the data and revised the paper; H.D., Y.L.S., J.L., Y.Y.Z., Z.H. L., C.W.G., E.C.D., X.L.C., X.H.B., X.Y., W.Y.M., Y.P.Z., X.K. J., R.B.C., P.C.Z., X.T., Y.J., Y.Z. participated in the experiments. All authors read and approved this manuscript.

Edited by: Yidan Ouyang, Huazhong Agricultural University, China

Received Jul. 26, 2022; **Accepted** Nov. 4, 2022; **Published** Nov. 4, 2022

REFERENCES

Andres-Colas, N., Zhu, Q., Takenaka, M., De, R.B., Weijers, D., and Van, D.S.D. (2017). Multiple PPR protein interactions are involved in the RNA editing system in *Arabidopsis* mitochondria and plastids. Proc. Natl. Acad. Sci. U.S.A. **114:** 8883–8888.

Barkan, A., and Small, I. (2014). Pentatricopeptide repeat proteins in plants. Annu. Rev. Plant Biol. **65:** 415–457.

Bonen, L. (2008). *Cis*- and *trans*-splicing of group II introns in plant mitochondria. Mitochondrion **8:** 26–34.

Braun, H.P., Binder, S., Brennicke, A., Eubel, H., Fernie, A.R., Finkemeier, I., Klodmann, J., KNig, A.C., Kühn, K., and Meyer, E. (2014). The life of plant mitochondrial complex I. Mitochondrion **19:** 295–313.

Brehme, N., Bayer-Császár, E., Glass, F., and Takenaka, M. (2015). The DYW subgroup PPR protein MEF35 targets RNA editing sites in the mitochondrial *rpl16*, *nad4* and *cob* mRNAs in *Arabidopsis thaliana*. PLoS ONE **10:** e0140680.

Bryant, N., Lloyd, J., Sweeney, C., Myouga, F., and Meinke, D. (2011). Identification of nuclear genes encoding chloroplast-localized proteins required for embryo development in *Arabidopsis*. Plant Physiol. **155:** 1678–1689.

Cai, M., Li, S., Sun, F., Sun, Q., Zhao, H., Ren, X., Zhao, Y., Tan, B.C., Zhang, Z., and Qiu, F. (2017). *Emp10* encodes a mitochondrial PPR protein that affects the *cis*-splicing of *nad2* intron 1 and seed development in maize. Plant J. **91:** 132–144.

Cai, W., Ji, D., Peng, L., Guo, J., Ma, J., Zou, M., Lu, C., and Zhang, L. (2009). LPA66 is required for editing *psbF* chloroplast transcripts in *Arabidopsis*. Plant Physiol. **150:** 1260–1271.

Cai, W., Okuda, K., Peng, L., and Shikanai, T. (2011). PROTON GRADIENT REGULATION 3 recognizes multiple targets with limited similarity and mediates translation and RNA stabilization in plastids. Plant J. **67:** 318–327.

Chateigner-Boutin, A.L., Colas, D.F.S.C., Fujii, S., Okuda, K., Tanz, S. K., and Small, I. (2013). The E domains of pentatricopeptide repeat proteins from different organelles are not functionally equivalent for RNA editing. Plant J. **74:** 935–945.

Chateigner-Boutin, A.L., Ramos-Vega, M., Guevara-Garcia, A., Andres, C., Gutierrez-Nava, M.D., Cantero, A., Delannoy, E., Jimenez, L.F., Lurin, C., Small, I., and León, P. (2008). CLB19, a pentatricopeptide repeat protein required for editing of *rpoA* and *clpP* chloroplast transcripts. Plant J. **56:** 590–602.

Chen, X., Feng, F., Qi, W., Xu, L., Yao, D., Wang, Q., and Song, R. (2017). *Dek35* encodes a PPR protein that affects *cis*-splicing of mitochondrial *nad4* intron 1 and seed dvelopment in maize. Mol. Plant **10:** 427–441.

Cohen, S., Zmudjak, M., Catherine, F.S., Malik, S., Shaya, F., Keren, I., Belausov, E., Many, Y., Brown, G.G., and Small, I. (2014). nMAT4, a maturase factor required for *nad1* pre-mRNA processing and maturation, is essential for holocomplexl biogenesis in *Arabidopsis* mitochondria. Plant J. **78:** 253–268.

Ding, Y.H., Liu, N.Y., Tang, Z.S., Liu, J., and Yang, W.C. (2006). *Arabidopsis* GLUTAMINE-RICH PROTEIN23 is essential for early embryogenesis and encodes a novel nuclear PPR motif protein that interacts with RNA polymerase II subunit III. Plant Cell **18:** 815–830.

Fujii, S., and Small, I. (2011). The evolution of RNA editing and pentatricopeptide repeat genes. New Phytol. **191:** 37–47.

Fujita, N., Yoshida, M., Kondo, T., Saito, K., Utsumi, Y., Tokunaga, T., Nishi, A., Satoh, H., Park, J.H., Jane, J.L., Miyao, A., Hirochika, H., and Nakamura, Y. (2007). Characterization of SSIIIa-deficient mutants of rice: The function of SSIIIa and pleiotropic effects by SSIIIa deficiency in the rice endosperm. Plant Physiol. **144:** 2009–2023.

Guillaumot, D., Lopez-Obando, M., Baudry, K., Avon, A., Rigaill, G., de Longevialle, A.F., Broche, B., Takenaka, M., Berthome, R., De Jaeger, G., Delannoy, E., and Lurin, C. (2017). Two interacting PPR proteins are major *Arabidopsis* editing factors in plastid and mitochondria. Proc. Natl. Acad. Sci. U.S.A. **114:** 8877–8882.

Han, J., Wang, X., Wang, F., Zhao, Z., Li, G., Zhu, X., Su, J., and Chen, L. (2021). The fungal effector *Avr-Pita* suppresses innate immunity by increasing COX activity in rice mitochondria. Rice **14:** 12.

Hao, Y., Wang, Y., Wu, M., Zhu, X., Teng, X., Sun, Y., Zhu, J., Zhang, Y., Jing, R., Lei, J., Li, J., Bao, X., Wang, C., Wang, Y., and Wan, J. (2019). The nuclear-localized PPR protein OsNPPR1 is important for mitochondrial function and endosperm development in rice. J. Exp. Bot. **70:** 4705–4720.

James, M.G., Denyer, K., and Myers, A.M. (2003). Starch synthesis in the cereal endosperm. Curr. Opin. Plant Biol. **6:** 215–222.

Johnson, X., Wostrikoff, K., Finazzi, G., Kuras, R., Schwarz, C., Bujaldon, S., Nickelsen, J., Stern, D.B., Wollman, F.A., and Vallon, O. (2010). MRL1, a conserved pentatricopeptide repeat protein, is required for stabilization of *rbcL* mRNA in *Chlamydomonas* and *Arabidopsis*. Plant Cell **22:** 234–248.

Kawagoe, Y., Kubo, A., Satoh, H., Takaiwa, F., and Nakamura, Y. (2010). Roles of isoamylase and ADP-glucose pyrophosphorylase in starch granule synthesis in rice endosperm. Plant J. **42:** 164–174.

Keren, I., Tal, L., Francs-Small, C., Araújo, W., Shevtsov, S., Shaya, F., Fernie, A.R., Small, I., and Ostersetzer-Biran, O. (2012). nMAT1, a nuclear-encoded maturase involved in the *trans*-splicing of *nad1* intron 1, is essential for mitochondrial complex I assembly and function. Plant J. **71:** 413–426.

Kim, S.R., Yang, J.I., Moon, S., Ryu, C.H., An, K., Kim, K.M., Yim, J., and An, G. (2009). Rice OGR1 encodes a pentatricopeptide repeat-DYW protein and is essential for RNA editing in mitochondria. Plant J. **59:** 738–749.

Lee, K., Ji, H.H., Park, Y., Francs-Small, C.C.D., Small, I., and Kang, H. (2017). The mitochondrial pentatricopeptide repeat protein PPR19 is involved in the stabilization of NADH dehydrogenase 1 transcripts and is crucial for mitochondrial function and *Arabidopsis thaliana* development. New Phytol. **215:** 202–216.

Li, X.J., Zhang, Y.F., Hou, M., Sun, F., Shen, Y., Xiu, Z.H., Wang, X., Chen, Z.L., Sun, S.S., Small, I., and Tan, B.C. (2014). *Small kernel 1* encodes a pentatricopeptide repeat protein required for mitochondrial *nad7* transcript editing and seed development in maize (*Zea mays*) and rice (*Oryza sativa*). Plant J. **79:** 797–809.

Liu, J., Wu, M.W., and Liu, C.M. (2022). Cereal endosperms: Development and storage product accumulation. Annu. Rev. Plant Biol. **73:** 255–291.

Liu, Y.J., Xiu, Z.H., Meeley, R., and Tan, B.C. (2013). *Empty pericarp5* encodes a pentatricopeptide repeat protein that is required for mitochondrial RNA editing and seed development in maize. Plant Cell **25:** 868–883.

Long, W., Wang, Y., Zhu, S., Jing, W., Wang, Y., Ren, Y., Tian, Y., Liu, S., Liu, X., and Chen, L. (2018). *FLOURY SHRUNKEN ENDOSPERM1* connects phospholipid metabolism and amyloplast development in rice. Plant Physiol. **177:** 698–712.

Longevialle, A.D., Meyer, E.H., Andrés, C., Taylor, N.L., Lurin, C., Millar, A.H., and Small, I.D. (2007). The pentatricopeptide repeat gene *OTP43* is required for *trans*-splicing of the mitochondrial *nad1* intron 1 in *Arabidopsis thaliana*. Plant Cell **19:** 3256–3265.

Lurin, C., Andrés, C., Aubourg, S.M.B., Bitton, F., Bruyère, C., Caboche, M., Debast, C., Gualberto, J., Hoffmann, B., Lecharny, A., Le, R.M., Martin-Magniette, M.L., Mireau, H., Peeters, N., Renou, J. P., Szurek, B., Taconnat, L., and Small, I. (2004). Genome-wide analysis of Arabidopsis pentatricopeptide repeat proteins reveals their essential role in organelle biogenesis. Plant Cell **16:** 2089–2103.

Peng, C., Wang, Y., Liu, F., Ren, Y., Zhou, K., Lv, J., Zheng, M., Zhao, S., Zhang, L., Wang, C., Jiang, L., Zhang, X., Guo, X., Bao, Y., and Wan, J. (2014). *FLOURY ENDOSPERM6* encodes a CBM48 domain-containing protein involved in compound granule formation and starch synthesis in rice endosperm. Plant J. **77:** 917–930.

Qi, W., Yang, Y., Feng, X., Zhang, M., and Song, R. (2017). Mitochondrial fFunction and maize kernel development requires Dek2, a pentatricopeptide repeat protein involved in *nad1* mRNA splicing. Genetics **205:** 239.

Ren, X., Pan, Z., Zhao, H., Zhao, J., Cai, M., Li, J., Zhang, Z., and Qiu, F. (2017). EMPTY PERICARP11 serves as a factor for splicing of mitochondrial *nad1* intron and is required to ensure proper seed development in maize. J. Exp. Bot. **68:** 4571–4581.

Robbins, J.C., Heller, W.P., and Hanson, M.R. (2009). A comparative genomics approach identifies a PPR-DYW protein that is essential for C-to-U editing of the *Arabidopsis* chloroplast *accD* transcript. RNA **15:** 1142–1153.

Shen, C.C., Zhang, D.L., Guan, Z.Y., Liu, Y.X., Yang, Z., Yang, Y., Wang, X., Wang, Q., Zhang, Q.X., Fan, S.L., Zou, T.T., and Yin, P. (2016). Structural basis for specific single-stranded RNA recognition by designer pentatricopeptide repeat proteins. Nat. Commun. **1:** 11258.

Small, I.D., Schallenberg-Rudinger, M., Takenaka, M., Mireau, H., and Ostersetzer-Biran, O. (2020). Plant organellar RNA editing: What 30 years of research has revealed. Plant J. **101:** 1040–1056.

Sun, F., Zhang, X., Shen, Y., Wang, H., Liu, R., Wang, X., Gao, D., Yang, Y. Z., Liu, Y., and Tan, B.C. (2018). The pentatricopeptide repeat protein EMPTY PERICARP8 is required for the splicing of three mitochondrial introns and seed development in maize. Plant J. **95:** 919–932.

Sun, T., Bentolila, S., and Hanson, M.R. (2016). The unexpected diversity of plant organelle RNA editosomes. Trends Plant Sci. **21:** 962–973.

Toda, T., Fujii, S., Noguchi, K., Kazama, T., and Toriyama, K. (2012). Rice *MPR25* encodes a pentatricopeptide repeat protein and is essential for RNA editing of *nad5* transcripts in mitochondria. Plant J. **72:** 450–460.

Toyosawa, Y., Kawagoe, Y., Matsushima, R., Crofts, N., Ogawa, M., Fukuda, M., Kumamaru, T., Okazaki, Y., Kusano, M., Saito, K., Toyooka, K., Sato, M., Ai, Y.F., Jane, J.L., Nakamura, Y., and Fujita, N. (2016). Deficiency of starch synthase IIIa and IVb alters starch granule morphology from polyhedral to spherical in rice endosperm. Plant Physiol. **170:** 1255–1270.

Waadt, R., and Kudla, J. (2008). In planta visualization of protein interactions using bimolecular fluorescence complementation (BiFC). CSH Protoc. **5:** pdb.prot4995.

Wang, C., Fabien, A., Noelya, P., Martine, Q., Céline, D., Fabien, N., and Hakim, M. (2017). The pentatricopeptide repeat protein MTSF2 stabilizes a *nad1* precursor transcript and defines the 3′ end of its 5′-half intron. Nucleic Acids Res. **10:** 6119–6134.

Wang, Y., Liu, X.Y., Yang, Y.Z., Huang, J., Sun, F., Lin, J.S., Gu, Z.Q., Sayyed, A., Xu, C.H., and Tan, B.C. (2019). *Empty Pericarp21* encodes a novel PPR-DYW protein that is required for mitochondrial RNA editing at multiple sites, complexes I and V biogenesis, and seed development in maize. PLoS Genet. **15:** e1008305.

Wang, Y., Li, H., Huang, Z.Q., Ma, B., Yang, Y.Z., Xiu, Z.H., Wang, L., and Tan, B.C. (2022). Maize PPR-E proteins mediate RNA C-to-U editing in mitochondria by recruiting the trans deaminase PCW1. Plant Cell https://doi.org/10.1093/plcell/koac298

Wu, M.M., Ren, Y.L., Cai, M.H., Wang, Y.L., Zhu, S.S., Zhu, J.P., Hao, Y.Y., Teng, X., Zhu, X.P., Jing, R.N., Zhang, H., Zhong, M. S., Wang, Y.F., Lei, C.L., Zhang, X., Guo, X.P., Cheng, Z.J., Lin, Q.B., Wang, J., Jiang, L., Bao, Y.Q., Wang, Y.H., and Wan, J.M. (2019). Rice *FLOURY ENDOSPERM10* encodes a pentatricopeptide repeat protein that is essential for the trans-splicing of mitochondrial *nad1* intron 1 and endosperm development. New Phytol. **223:** 736–750.

Xiao, H.J., Zhang, Q.N., Qin, X.J., Xu, Y.H., Ni, C.Z., Huang, J.S., Zhu, L. L., Zhong, F.Y., Liu, W., Yao, G.X., Zhu, Y.G., and Hu, J. (2018). Rice *PPS1* encodes a DYW motif-containing pentatricopeptide repeat protein required for five consecutive RNA-editing sites of *nad3* in mitochondria. New Phytol. **220:** 878–892.

Yan, J., Yao, Y., Hong, S., Yang, Y., Shen, C., Zhang, Q., Zhang, D., Zou, T., and Yin, P. (2019). Delineation of pentatricopeptide repeat codes for target RNA prediction. Nucleic Acids Res. **47:** 3728–3738.

Yang, Y.Z., Ding, S., Wang, H.C., Feng, S., and Tan, B.C. (2017). The pentatricopeptide repeat protein EMP9 is required for mitochondrial *ccmB* and *rps4* transcript editing, mitochondrial complex biogenesis and seed development in maize. New Phytol. **214:** 782.

Yang, Y.Z., Liu, X.Y., Tang, J.J., Wang, Y., Xu, C., and Tan, B.C. (2022). GRP23 plays a core role in E-type editosomes via interacting with MORFs and atypical PPR-DYWs in *Arabidopsis* mitochondria. Proc. Natl. Acad. Sci. U.S.A. **119:** 39–48.

Yin, P., Li, Q.X., Yan, C.G., Liu, Y., Liu, J.J., Yu, F., Wang, Z., Long, J.F., He, J.H., Wang, H.W., Wang, J.W., Zhu, J.K., Shi, Y.G., and Yan, N. (2013). Structural basis for the modular recognition of single-stranded RNA by PPR proteins. Nature **7478:** 168–171.

Zhang, Z., Cui, X., Wang, Y., Wu, J., Gu, X., and Lu, T. (2017). The RNA editing factor WSP1 is essential for chloroplast development in rice. Mol. Plant **10:** 86–98.

Zhu, Q., Dugardeyn, J., Zhang, C.Y., Takenaka, M., Kuhn, K., Craddock, C., Smalle, J., Karampelias, M., Denecke, J., Peters, J., Gerats, T., Brennicke, A., Eastmond, P., Meyer, E.H., and Van, D.D. S. (2012). SLO2, a mitochondrial pentatricopeptide repeat protein affecting several RNA editing sites, is required for energy metabolism. Plant J. **71:** 836–849.

Zsigmond, L., Szepesi, A., Tari, I., Rigó, G., Király, A., and Szabados, L. (2012). Overexpression of the mitochondrial *PPR40* gene improves salt tolerance in *Arabidopsis*. Plant Sci. **182:** 87–93.

SUPPORTING INFORMATION

Additional Supporting Information may be found online in the supporting information tab for this article: http://onlinelibrary.wiley.com/doi/10.1111/jipb.13402/suppinfo

Dataset S1. Pentatricopeptide repeat (PPR) proteins in rice

Dataset S2. Differentially expressed genes (DEGs) in wild type and *flo22* from results of high-throughput RNA sequencing (RNA-seq)

Dataset S3. Gene Ontology (GO) classification of differentially expressed genes (DEGs) in wild type and *flo22*

Dataset S4. Kyoto Encyclopedia of Genes and Genomes (KEGG) pathway enhancement of differentially expressed genes (DEGs) in wild type and *flo22*

Figure S1. Comparison of major agronomic traits of wild type and the *flo22* mutant

Figure S2. Plant heights of wild type, *flo22* mutant, and transgenic complementary lines

Figure S3. Phylogenetic tree and amino acid sequence alignment of FLOURY ENDOSPERM22 (FLO22) and its homologs

Figure S4. RNA-seq analysis showing that the messenger RNA levels of starch and sucrose metabolism-related genes and multiple biological process-related genes that function in mitochondria were disrupted in the *flo22* mutant

Figure S5. Yeast two-hybrid assays for possible factors interacting with FLOURY ENDOSPERM22 (FLO22)

Figure S6. *dyw3* clustered regularly interspaced palindromic repeats (CRISPR)/CRISPR-associated nucleotide 9 (Cas9) knockdown lines had reduced editing efficiency of several mitochondrial sites and impaired plant growth

Figure S7. Schematic model for the role of FLOURY ENDOSPERM22 (FLO22) in plant growth and endosperm development

Table S1. Primers used in this study

Table S2. Prediction of pentatricopeptide repeat (PPR) binding site

Table S3. The obtained recognition motif was used to scan the mitochondria genome from the National Center for Biotechnology Information

Table S4. Analysis of all known mitochondrial editing sites in wild type and *flo22* mutant

Table S5. The obtained recognition motif was used to scan the *nad9* transcript

Scan using WeChat with your smartphone to view JIPB online

Scan with iPhone or iPad to view JIPB online